Dynamics and kinetics of molecular high Rydberg states in the presence of an electrical field: An experimental and classical computational study

Eran Rabani, R. D. Levine, Annette Mühlpfordt, and U. Even

Citation: The Journal of Chemical Physics **102**, 1619 (1995); doi: 10.1063/1.468894
View online: http://dx.doi.org/10.1063/1.468894
View Table of Contents: http://scitation.aip.org/content/aip/journal/jcp/102/4?ver=pdfcov
Published by the AIP Publishing

Dynamics and kinetics of molecular high Rydberg states in the presence of an electrical field: An experimental and classical computational study

Eran Rabani and R. D. Levine
The Fritz Haber Research Center for Molecular Dynamics, The Hebrew University, Jerusalem 91904, Israel

Annette Mühlpfordt[a] and U. Even
School of Chemistry, Sackler Faculty of Exact Sciences, Tel Aviv University, Tel Aviv 69984, Israel

(Received 16 June 1994; accepted 13 October 1994)

The effect of an electrical field on the dynamics and decay kinetics of a high Rydberg electron coupled to a core is discussed with special reference to simulations using classical dynamics and to experiment. The emphasis is on the evolution of the system within the range of Rydberg states that can be detected by delayed pulsed ionization spectroscopy (which is $n>90$ for both the experiment and the computations). The Hamiltonian used in the computations is that of a diatomic ionic core about which the electron revolves. The primary coupling is due to the anisotropic part of the potential which can induce energy and angular momentum exchange between the orbital motion of the electron and the rotation of the ion. The role of the field is to modulate this coupling due to the oscillation of the orbital angular momentum l of the electron. In the region of interest, this oscillation reduces the frequency with which the electron gets near to the core and thereby slows down the decay caused by the coupling to the core. In the kinetic decay curves this is seen as a stretching of the time axis. For lower Rydberg states, where the oscillation of l is slower, the precession of the orbit, due to the central but not Coulombic part of the potential of the core, prevents the oscillation of l and the decay is not slowed down. Examination of individual trajectories demonstrates that the stretching of the time axis due to the oscillatory motion of the electron angular momentum in the presence of the field is as expected on the basis of theoretical considerations. The relation of this time stretch to the concept of the dilution effect is discussed, with special reference to the coherence width of our laser and to other details of the excitation process. A limit on the principal quantum number below which the time stretch effect will be absent is demonstrated by the computations. The trajectories show both up and down processes in which the electron escapes from the detection window by either a gain or a loss of enough energy. Either process occurs in a diffusive like fashion of many smaller steps, except for a fraction of trajectories where prompt ionization occurs. The results for ensembles of trajectories are examined in terms of the decay kinetics. It is found that after a short induction period, which can be identified with the sampling time of the available phase space, the kinetics of the decay depend only on the initial energy of the electron and on the magnitude of the field, but not on the other details of the excitation process. The computed kinetics of the up and down channels are shown to represent competing decay modes. A possible intramolecular mechanism for long time stability based on the sojourn in intermediate Rydberg states is discussed. The available experimental evidence does not suffice to rule out nor to substantiate this mechanism, and additional tests are proposed. The theoretical expectations are discussed in relation to observed time resolved decay kinetics of high Rydberg states of BBC (bisbenzenechromium) and of DABCO (1,4-diazabicyclo[2.2.2]octane). The experimental setup allows for the imposition of a weak (0.1–1.5 V/cm) electrical field in the excitation region. The role of the amplitude of the time delayed field, used to detect the surviving Rydberg states by ionization, is also examined. The observed decay kinetics are as previously reported for cold aromatic molecules: Most of the decay is on the sub-μs time scale with a minor ($\sim$10%) longer time component. The decay rate of the faster component increases with the magnitude of the field. Many features in such an experiment, including the absolute time scales, are similar to those found in the classical trajectory computations, suggesting that the Hamiltonian used correctly describes the physics of the faster decay kinetics of the high Rydberg states. © *1995 American Institute of Physics.*

I. INTRODUCTION

Current experimental interest in very high (principal quantum number $n\geqslant 100$) molecular Rydberg states is made possible by ZEKE (zero electron kinetic energy) spectroscopy.[1–3] For a theorist, these states provide a new coupling regime where the orbital period of the electron ($\tau\cong 1.52\ 10^{-16}\ n^3$ s) is longer than even the rotational periods of most molecules. The new time scale brought into the problem by the presence of a weak dc electrical field is the period of the oscillation of the orbital angular momentum of the

[a]Permanent address: Max Planck Institute for Biophysical Chemistry, Gottingen, Germany.

electron in the presence of a dc field.[4] Under typical conditions, the period of this oscillation is even slower than that of the orbital motion and at lower n's it can be slower than even the precession of the orbit.

One expects high Rydberg states to live long. There is an active discussion whether, on an experimentally realistic, sub-μs time scale, such states can decay by intramolecular coupling[5] or will they be so stable that any observed decay must be due to the ultimately unavoidable external perturbations.[6–8] By their very size, (the semimajor axis of the orbit equals n^2 in atomic units), high Rydberg states are a very sensitive probe of their surroundings[9,10] so that an induced decay can be readily established. In this paper we report on a joint experimental-computational study on the role of a dc field on the dynamics at high n's. The present work was not undertaken for the purpose of resolving the question of the origin of the, recently often commented upon,[1–3,6–8,11] longer time (μs scale) stability of such states, and is primarily concerned with the, so-called,[5,12,13] short time decay.

Time resolved experiments[5,12–14] on the decay kinetics of high Rydberg states of cold aromatic molecules have uncovered two time regimes. A major component which decays on a sub-μs time scale and a smaller ($\sim$10%) component with a few μs's decay time. There was a time delay of at least 100 ns between excitation and the start of detection, caused by the need to remove any promptly produced charged particles. Two quite different experimental setups were used. A magnetic bottle arrangement[14–16] and a simple two parallel plates arrangement.[17] The rate of the decay was too fast (i.e., sub-100 ns) to accurately measure up to about 20 cm^{-1} below the threshold to ionization. At higher energies, the decay rate decreased as the threshold was approached but took an upturn just below threshold. The result is a bell-shaped lifetime vs frequency plot which has been reported[5] for phenanthrene and its deuterated analog. Essentially similar results were obtained for a number of other aromatics [Aniline, DCA (9,10 di chloroanthracene), indole, perylene, tetracene]. More recently,[13] these measurements were repeated for two molecules (BBC and DABCO) for which a Rydberg series at much lower energies could be determined so that a fit to the Rydberg term formula[4] provided an independent determination of the ionization potential and thereby of the value of n for states just below the threshold. The results[13] on BBC and DABCO also raised the possibility that the observed short time decay of Rydberg states of high n's, (say $n>100$) is significantly slower than could be expected by extrapolation of the observed widths of the lower n states. Our theoretical considerations below will suggest that this demarcation between the dynamics of intermediate and high n's is to be expected but that a fraction of the decays should be faster, i.e., on the same time scale as expected from the extrapolation. This very fast decay is, however, on the borderline of what can be monitored by the present experimental setups.

The previously observed short time decay of the high Rydberg states of the cold aromatic molecules is on the same time scale and shows other common characteristics with the decay curves of BBC and of DABCO. Yet there is an important experimental difference. The aromatic molecules as well as BBC are cold (the rotational temperature, estimated from the rotational envelope of the spectrum of the S_1 intermediate state is below 4 K). For a photon energy just below the threshold for ionization, the energy required for the electron to ionize must be provided by the core. The Rydberg states of DABCO are pumped via a vibrationally excited states of the S_1 intermediate, so that the energy of the core is higher. However, on the short time scale, one does not discern any different behavior. Elsewhere we shall also report in detail that the short time decay kinetics of DABCO are essentially independent of which vibrational state of the S_1 intermediate is used. We have carried many experimental checks in order to insure that the short decay is not collision induced. The results of the simulations, as reported below, are an additional check.

A technical point, but one that is central to our interpretation of the experimental results, is what is measured in a time resolved ZEKE experiment. Since the detection is by ionization due to a delayed pulsed field, it is all those Rydberg states that can be ionized by the applied field, irrespective of their initial value of n, that are detected. We shall refer to this range of states as ''the detection window.'' The measured decay kinetics do not determine the rate to exit from the initially accessed value of n. Rather, what is measured is the decay of the population within the detection window. The two decay rates can be quite different[18] and it is this difference that motivates our model Hamiltonian and provides the reason why we consider that it is relevant to the decay dynamics of larger molecules. The point is that the exit from the initial value of n can be significantly faster than the exit from the detection window, which spans a range of high n values. The sampling of these high n states is enhanced by the anisotropy of the core, provided that it has a low rotational constant. Energy exchange with a core of high rotational constant [e.g., Ref. 19(b)], H_2 and/or with the vibrations, (or, in the case of atoms, with an electronically excited core[8(b)]) can remove the Rydberg electron from the detection window in one step, and, of course, such an exit is due to ionization, i.e., up. The simulations do show such processes and they are typically very fast. In this, and a previous study,[18] we are equally concerned with the diffusivelike motion of the Rydberg electron amongst the high n states prior to its ultimate exit from the detection window. This exit can be either up or down. The dynamics and the decay kinetics that are the subject of this paper are those that refer to this two way exit, which we compute to be on the same, fast, time scale as that seen in the experiments.[5,12–14] Not included in our simulations is a possible role of other ions in inducing a decay of the Rydberg state.

The presence of a dc field slows down the sampling of the states in the detection window and is one of the main topics of this paper. Mechanistically, this slowing down is due to the reduced frequency with which the electron can get near to the core. This effect will be equally operative whether the electron couples to the core and exits from the detection window in one step or whether the coupling to the core induces a smaller change in n and the electron remains in the

detection range longer. Our theoretical considerations regarding the role of the field are thus applicable also to such systems where the exit from the detection window is in one step. However, the simulations to be presented center attention on a diffusivelike exit from the detection window, which we consider to be typical for larger molecules. We have performed simulations also for the case of larger energy exchanges with the core, and these will be reported elsewhere.

A component exhibiting longer time decay ($>\mu$s's) of Rydberg states of larger molecules was reported by several groups[7,8,11,20–24] and short time decay has been measured for diatomic molecules[19,25] but, so far, no independent measurements of the short time kinetics have been reported for large molecules. Indeed, the initially reported[5] results on the short time evolution were questioned[6,7] as being possibly due to external perturbations. We have undertaken a classical trajectory study of the short time kinetics[18,26] with the aim of determining the time scale for the intramolecular decay under realistic experimental conditions. The independent determination[13] (from the series of lower Rydberg states) of the ionization potential for BBC, enables us to state that the energy of the photon is below the threshold for ionization. If intramolecular ionization of the cold molecule does take place, the required energy is that initially present as a rotation. For this reason, the time scale should be similar to that of a diatomic molecule, but a diatomic molecule with a lower rotational constant (as expected for a large polyatomic). The additional isoenergetic channels present in a polyatomic molecule are those where the core is vibrationally excited, with the Rydberg electron being in lower n states. We consider that these channels do contribute,[12,27] particularly at longer times, and further discuss this possibility below.

In this paper we report on a joint experimental and theoretical study, where the magnitude of the, otherwise stray, dc field is varied in a controlled fashion. The experimental setup is as previously discussed[13] so that only the results will be reported and much of the paper is devoted to theoretical considerations. These cover diverse aspects of the kinetics and dynamics of high Rydberg states and provide a possible interpretation of the experimental results, an interpretation which is supported by a computational study. In future work we intend to provide experimental tests of other points (in particular, the role of the detection window, the lower end of the time stretching regime, the mechanism of the long time stability and on the possibility of an even earlier, sub-100 ns, dynamical regime) made in the theoretical discussion. Other experimental work in progress, including the role of a magnetic field, is mentioned, where appropriate, in the text.

The theoretical considerations use classical mechanics to monitor the time evolution of an initially excited state. We suggest that the prime limitation of this approach is in the description of the initial state. One can, and should, worry about coherence effects in the excitation process and we will discuss this point in detail. Otherwise, the limitation of classical mechanics is not so much in the description of the dynamics of the electron as in that of the rotational degrees of freedom of the molecule. A special attention will be paid to the unavoidable experimental reality, namely, that the states are typically not produced in a strictly field free space. The Hamiltonian used explicitly includes a (so-called, ''weak'') dc electrical field. (The field is not really weak because the relevant parameter is[28] the field multiplied by n^4). One can argue that this, sometimes known as ''stray,'' field should be regarded as an external perturbation. The essential physical point is however that the presence of a field of realistic strength makes the magnitude of the orbital angular momentum of the electron oscillate in an almost harmonic motion with a frequency that is not small compared to the orbital period of the electron.

There is a rich literature dealing with the dynamics of far lower Rydberg states.[29–39] We are cognizant of this incisive contribution, yet we do not consider that the results and the important insights that have been provided can be simply extrapolated to the regime of high n's of larger molecules. One reason that we already mentioned is that we are interested in the dynamics within the detection window, a process which requires coupling to low frequency motions of the core. The rates of exit that are here computed are thus very much not the same as the rate of exit from the initially excited state. It is only the coupling to the higher frequency motions of the core which can cause a one step exit. The reason is the rather steep n dependence of the frequency of the electronic motion. The spacing of adjacent states is $2R/n^3$ or about $2.19\times10^5\cdot n^{-3}$ cm^{-1} and while at lower n's this can be comparable to even vibrational frequencies, (or to spin orbit couplings[8(b)]), at the high n's of interest it can be lower even compared to rotational spacing. Nonlinear mechanics[40,41] has reiterated the familiar result[42] that frequency matching is an important ingredient for effective coupling of different modes. (This is sometimes referred to as the ''exponential gap rule''). In the regime of high n's one cannot insure a 1:1 (or other low order) frequency matching. In the language of nonlinear mechanics, it is the higher order resonances that determine the dynamics. This is well known to confer stability with the most familiar example being the long lifetimes of van der Waals molecules[43,44] where the analogy is between the low frequency van der Waals bond and the high n electron. We will return below to the role of the vibrations of the core, but the primary emphasis in this paper is on the first exit of the electron from the detection window, without regard to its ultimate fate.

The analysis of the dynamics in this paper is based on a Hamiltonian description. It is therefore possible, in principle, to establish a correspondence with the terminology used in a quantum mechanical configuration interaction type of description.[3,8(c),31,32,34–38,45–47] The primary point is that the quantal analog of our trajectory computations is a basis set which spans a wide range of n values (from the bottom of the detection window at $n=90$ and up. The upper limit is determined by the onset of ionization due to the dc field present in the excitation region). The exit from the detection window that we call up is an autoionization process. The trajectory computations in the absence of the field[18] do, however, show that, apart from a fraction of prompt exits, the initially excited state is very significantly mixed with other n states prior to its ionization. Examination of individual trajectories shows that both higher and lower values of n are visited prior to the ultimate exit. In the language of configu-

ration interaction, we find extensive channel–channel couplings. So much so, that after an induction period, which will be discussed in detail below, the evolution in n looks diffusivelike. The field can cause a further dilution[34] by mixing in higher l states. In the time dependent language that is appropriate to a trajectory computation, this leads to a further stretching of the time axis, as will be discussed in detail.

We shall also argue that another aspect which distinguishes the high n limit is that the rate of precession of the Rydberg orbit, due to the core potential not being quite Coulombic, slows down as n increases and that this has a qualitative effect on the resulting dynamics. The predicted boundary between the high and lower n regimes turns out to depend on the magnitude of the dc field and will be discussed with computational examples.

Section II provides the details of the Hamiltonian and of the action-angle variables we use to insure the numerical stability of the integration over many periods. This stability is particularly important when the molecule is allowed to vibrate so that the time step is determined by the vibrational period, which is several orders of magnitude faster than the orbital period of the electron. The action variables are constants of the motion for a particular zeroth order Hamiltonian but do change in time due to the coupling between the electron and the rotation and vibration of the ionic molecular core. Two alternative sets of action variables are used for the electron. The first, is the more familiar kind[4,48,49] which are the classical analogs of the usual three quantum numbers of an electron moving in a Coulomb potential. These change in time not only due to the potential of the core not being purely Coulombic but also because of the presence of a dc electrical field. We also use the, so-called, parabolic action variables[4,48] which are constant in time also in the presence of the field and change only due to the coupling to the core. The second set of action variables should, in principle, provide a better numerical stability. In practice, the advantage is marginal since the change in l, due to the presence of the dc field, is slow. The prime use we make of these variables is to provide an interpretation of the role of the field. Another key point introduced in Sec. II is the specification of the, so-called, detection window. This is the range of n values which is probed by the ZEKE-type[1–3] detection setup. In other words, Rydberg states can, in principle, decay by one of two intramolecular routes. The Rydberg electron can autoionize or it can lose so much energy to the core that its instantaneous value of n is so low that it will not be ionized by the external delayed field employed to detect any surviving Rydberg states.[5]

On the basis of a kinetic analysis, we have previously suggested[12] that the long time stability of the isolated molecule can be due to some of those electrons that have gone down in n, below the threshold for detection, coming up in n at much longer times. The results of the simulations support this as a possible mechanism. Another way to think about this mechanism is as a limiting case of vibrational autoionization of low Rydberg states. It is well known that low lying Rydberg states of a vibrationally excited diatomic core can autoionize and there are extensive studies of the rate of such processes.[3,27,29–32,37,50–53] This is also seen in polyatomic molecules[33] and in the autodetachment of negative ions.[54] The only difference is that we are concerned with the promotion of the electron to the quasicontinum of Rydberg states rather than to the real continum of a free electron, and it is known[55] that matrix elements of the relevant type can be extrapolated across the threshold. This does not mean that long time stability cannot be conferred by external perturbations.[6,7] It only means that there may be also a purely intramolecular mechanism for this stability. Indeed, there is more than one such mechanism. Another type of trajectory which can survive into the μs time scale is that of exceedingly high n's, where the orbital periods are very long, which fail to ionize even though they are above the threshold for ionization in the presence of a weak stray dc electrical field. (These are the analogs of the atomic ''Stark states'' above the ionization threshold[56,57] with the important difference that here these states ionize because of the anisotropy of the core).

Section III examines the detailed dynamics. Particular attention is given to the role of the external stray dc field in determining the time evolution of the angular momentum of the electron. We do not agree with the suggestions in the literature that this is the origin of the long time stability. It is certainly the case that electrons with higher angular momentum do not couple effectively to the electrical anisotropy of the core. Since the point of closest approach of a hydrogenic electron is $\approx l(l+1)/2$ (for $l<n$) in atomic units away from the core, it is not even necessary to have a very high l for the electron to see only the spherical part of the potential and to be otherwise decoupled from the core. A quite moderate value of l will suffice. It is also the case that a dc field will drive an initially low angular momentum of the electron to higher values. The essential point is however that while l will initially increase it will then reach a maximal value (which, depending on m_l, can be as high as n) and proceed to decrease all the way back. It will continue in this periodic motion (which, to first order, is harmonic with a frequency, in atomic units, of[26] $3Fn$, where F is the field), thereby enabling the electron to periodically get near the core. What the presence of the field does de facto do is to reduce the frequency with which the electron can effectively couple to the molecular core.[26] This causes an elongation of the decay time and we shall put a quantitative measure on it in Sec. III. The dc field effect on l does not however suffice for confering long time stability.

The slowing down of the decay of high Rydberg states by a stray dc field has both an upper and a lower n limit. The upper limit occurs due to the increase with n of the frequency of the oscillation in l. Once this frequency begins to approach the orbital period of the electron, the importance of the effect is much reduced. The lower limit is due to the precession of the orbit of the electron. The other aspect of the dynamics to be discussed in detail in Sec. III, is the interpretation of the motion using the parabolic action variables.

Section IV provides the details of the experimental and the computed decay kinetics. The experiment only measures the total decay rate (for times longer than 100 ns) and we compare the magnitude and the dc field dependence of this rate with the computed results. For the short, sub μs, decay,

the agreement is close. Since no attempt was made to insure the agreement and the computations preceded the experiment, we take the agreement to suggest that the short time decay can be due to the proposed mechanism. The role of the vibrational degrees of freedom of BBC [bis(benzene)chromium] or of DABCO, which can lead to predissociation of the neutral molecule is then manifested only after the electron exited from the detection window, that is on a longer timescale than the short decay. We discuss also the component exhibiting longer, μs scale, decay which is not well reproduced by the computations which center attention on the first exit from the detection window. We present some very tentative conclusions that it is here that the role of the vibrations will be manifested. More work on this point is in progress. The computational results in Sec. IV also demonstrate that both the up and the down decay channels[5] are important and that the rates of the two processes do vary with frequency in opposite directions. The results also show the presence of a sub 100 ns induction period during which a simple kinetic analysis is inappropriate and the decay is sensitive to the initial conditions of the trajectory. This is only to be expected, as it must take several orbital periods for the electron to decay in a manner which depends only on the initial value of its action variables and not on the angle variables. We very much intend to examine this point using faster lasers and detection.

Section V is a discussion of the implications of the present results for the long term stability of high molecular Rydberg states. The available experimental results on the role of the delayed electrical field used to detect the surviving Rydberg states are also discussed therein. Section VI is an overall summary.

II. THEORETICAL PRELIMINARIES

This section defines the Hamiltonian and the action-angle variables and specifies other relevant details. In particular, the technical specification of what we mean by the detection window is provided in subsection D.

A. Hamiltonian

The Hamiltonian used in the simulation is that of an electron moving in a field of an anisotropic ion in the presence of an external dc electrical field. The field about the center of charge of the ion has both a central, spherically symmetric term and additional, anisotropic contributions from the higher multipoles of the ion. The main contribution to the central potential is a Coulombic term but we also include a shorter range contribution which describes the precession of the electronic orbit and gives rise to a quantum defect.[4] The electron is coupled to the rotation of the core because of the anisotropic part of the potential. The electrical multipole moments (dipole, quadrupole) of the core are taken to be functions of the vibrational coordinate of the diatomic core and thereby the vibrational motion is also coupled to that of the electron. The molecular core itself is taken to be a rigid rotor-anharmonic vibrator. In all the simulations reported in this paper, the core has initially only the zero point energy in its vibration so that the role of the anharmonicity is primarily electrical, in that the multipoles depend nonlinearly on the vibrational coordinate. The dc electrical field is taken in the z direction. Using low case letters for the Cartesian coordinates of the electron and large case letters for the core, the Hamiltonian, in atomic units, for a dipolar anisotropy, has the form

$$H=H_e+H_m+V+F\cdot z. \tag{2.1}$$

$$H_e=(\mathbf{p}^2/2)-(1/\mathbf{r}), \tag{2.2}$$

$$H_m=Bj^2+P^2/2m+D_e(1-\exp(-\beta(R-R_e)))^2$$
$$=Bj^2+\beta^{-1}(2D_e/m)^{1/2}i-(\beta^2/2m)i^2, \tag{2.3}$$

$$V=(\mu(R)/r^2)\cdot\cos(\chi)+C_2/r^2. \tag{2.4}$$

Here, H_e is the Hamiltonian for a hydrogeniclike electron and the non-Coulombic part of the central potential is included in V. The Hamiltonian of the isolated ionic core is H_m where B is the rotational constant ($B=0.15$ cm^{-1}). m is the reduced mass of the ionic core, $m=11.5$ amu. The vibrational potential is Morse, with a depth $D_e=0.036$ a.u. and a range $\beta=0.31$ a.u. j and i are the action of the rotation and vibration (in units of $\hbar$). The coupling of the hydrogeniclike electron to the core is described by V. The anisotropy, as written, includes only the leading term where $\mu(R)$ is the R-dependent dipole moment

$$\mu(R)=\mu_0+\mu_1\left(\frac{\partial U(R)}{\partial R}\right). \tag{2.5}$$

U is the Morse potential function of Eq. (2.3) and $\mu_0=0.3$ a.u. The anisotropic coupling depends on the angle χ between the two dipoles, the electronic one (in the direction $\hat{\mathbf{r}}$) and that of the ionic core (in the direction $\hat{\mathbf{R}}$). We have also used a quadrupolar term but found no essential differences whether that term is used as the leading contribution or in conjunction with a dipole. All the other terms in the Hamiltonian conserve the projection quantum number m_j of the core angular momentum j. The dipolar term can change m_j by ±1 whereas the quadrupolar coupling can change it by ±2. The last term in Eq. (2.1) is the coupling to the dc field of strength F.

The Hamiltonian equations of motion were integrated using a Gear six order predictor-corrector method[58] with a variable time step procedure fashioned after that typically used[59] for the Runge–Kutta integrator. The use of a variable time step enables us to slow down the integration when the electron is near its perihelion where it is strongly perturbed by the shorter range anisotropic coupling to the core. Otherwise we take advantage of the action-angle variables, as described below, to take much larger time steps.

B. Action-angle variables

The electron is only effectively coupled to the core when it is near its point of closest approach. At high n's, this lasts for but a very short fraction of the orbital period. For almost all the time the electron and the core are uncoupled. It therefore makes practical sense to use such variables that take advantage of this aspect of the dynamics. The other argument against using the usual geometrical variables such as the radius vector of the electron is their rather wide dynamic

range. There are two possible choices for action angle variables. The first is the good (i.e., conserved) variables of the first two terms in Eq. (2.1). These are the familiar[4,48,49] action angle variables of the hydrogeniclike electron and, for the core, the vibrational action[49] of the Morse oscillator, the angular momentum and its projection and their angle variables. We use the same notation for action variables as for the corresponding quantum numbers (e.g., l for the angular momentum of the electron) and denote the angle variables as α with a subscript identifying the conjugate action variable. The details are available elsewhere[18,49] and are given, for completeness, in Appendix A.

Not quite so familiar are the action variables for the hydrogenic electron in the presence of a dc field.[4,48] These are the so-called parabolic action variables.

In the presence of a dc field, a hydrogenic electron can, in classical mechanics, ionize at lower energy than when the field is absent. It does not however follow that an electron with energy above that threshold will necessarily ionize. The prime advantage that we find in using the parabolic variables is that this point is clearly evident when these are used. This is due to the difference in the kind of motion that is described by the two action variables[4,28] I_η and I_ξ which replace the hydrogenic variables n and l. The motion for which ξ is the coordinate is in a bound potential. There is no escape of the electron. Not so for the motion along the η coordinate. If the energy is high enough, the electron will ionize. In the presence of a field

$$I = I_\eta + I_\xi + |m_i|. \tag{2.6}$$

To first order in the field strength, the energy, in atomic units, of the electron is given by

$$E = -(1/2I^2) - (3/2)I(I_\xi - I_\eta)F \tag{2.7}$$

showing the respective role of η and ξ.

The relation between the parabolic and hydrogenic action variables that we use is that computed by Born[4] and is given in Appendix B. We have verified that in the absence of coupling to the core, and for the field strengths of interest to us (say <1.0 V/cm), the action variables, defined by the first order approximation of Appendix B, are very well conserved. A further check was the conservation of the constant of motion **b** (Runge–Lenz vector), as defined in problem 1, section 48 of Ref. 48.

Initial conditions for a classical trajectory require not only the values of the actions but also of the conjugate angle variables. For a particular set of parabolic initial conditions, the angular momentum, l, of the electron has a sharp value. As one keeps the parabolic actions constant and varies the angle variables, cf. Sec. II C below, the value of l will change. Quantum mechanically,[60] an initial state specified by the parabolic quantum numbers corresponds to a distribution over values of l.

The coupling term V in the Hamiltonian (2.1) depends on both action and angle variables. Written explicitly in terms of the hydrogenic action-angle variables, and the orientation angle ψ of r with respect to the major axis of the ellipse [cf. Eq. (2.11) below], the angle between the position vector of the electron and the axis of the diatomic ionic core has the form

$$\begin{aligned}\cos(\chi) = {} & \sin(\alpha_j)\sin(\alpha_{mj})\sin(\psi+\alpha_l)\sin(\alpha_{ml}) + \sin(\alpha_j)\cos(\alpha_{mj})\sin(\psi+\alpha_l)\cos(\alpha_{ml}) - \sin(\alpha_j)\sin(\alpha_{mj}) \\ & \times\cos(\psi+\alpha_l)\cos(\alpha_{ml})\cos(\beta_l) + \sin(\alpha_j)\cos(\alpha_{mj})\cos(\psi+\alpha_l)\sin(\alpha_{ml})\cos(\beta_l) - \cos(\alpha_j)\cos(\alpha_{mj}) \\ & \times\sin(\psi+\alpha_l)\sin(\alpha_{ml})\cos(\beta_j) + \cos(\alpha_j)\sin(\alpha_{mj})\sin(\psi+\alpha_l)\cos(\alpha_{ml})\cos(\beta_j) + \cos(\alpha_j)\cos(\alpha_{mj}) \\ & \times\cos(\psi+\alpha_l)\cos(\alpha_{ml})\cos(\beta_j)\cos(\beta_l) + \cos(\alpha_j)\sin(\alpha_{mj})\cos(\psi+\alpha_l)\sin(\alpha_{ml})\cos(\beta_j)\cos(\beta_l) \\ & + \cos(\alpha_j)\cos(\psi+\alpha_l)\sin(\beta_j)\sin(\beta_l).\end{aligned} \tag{2.8}$$

where

$$\cos(\beta_j) = m_j/j, \tag{2.9}$$

$$\cos(\beta_l) = m_l/l. \tag{2.10}$$

The position of the electron r, is related to ψ by the standard polar representation of an ellipse (where ϵ_n is the eccentricity) with the origin at its focus

$$r = \frac{n^2(1-\epsilon_n)}{1-\epsilon_n\cos(\psi)}. \tag{2.11}$$

C. Initial conditions

The semiclassical correspondence between action variables and quantum numbers simplifies the specification of initial conditions. To mimic an initial quantum mechanical state which is an eigenstate of a zeroth order Hamiltonian H_0 we generate an entire ensemble of trajectories. The different trajectories all have the same set of initial values of the action variables of H_0 and these match the desired values of the quantum numbers. To facilitate this step we measure and report classical action variables in units of $\hbar$ so that the two sets are numerically identical. The different trajectories of the ensemble differ in the initial values of the angle vari-

ables. These are randomly chosen using a Monte Carlo procedure. We typically use at least 200 trajectories to mimic given quantal initial conditions.

There are two simple choices for the choice of zeroth order Hamiltonian H_0 which specifies the initial state. Each offers its own advantages and the decision which one is more convenient depends also on the experimental details of the initial excitation process. It is at this point that essential questions about quantal interference effects come in. Before we turn to the discussion of what can be, we anticipate and report on what is. For our laser coherence width (ca. 10^{-2} cm^{-1}), and for the range of n values (say 100–200) and electrical field strengths, F, (0.1–1 V/cm) of interest, and on the relevant time scales (>100 ns), one can, just as well, use hydrogeniclike initial conditions. These consist of the usual hydrogenic quantum numbers for the electron and rovibrational quantum numbers for the core. This is not to deny that there cannot be other limits, (particularly so, because of the strong scaling with n, at far lower n values and, otherwise, for far shorter laser pulses). It remains however for the experiment to show that these other limits can be realized.

The first consideration applies even in the absence of a dc field. The orbital period of the electron is quite long. Is the coherent excitation time of the laser sufficient to pump a stationary Rydberg state or does it create an electronic wave packet spanning several n states?[61] The same question in the frequency domain is whether the coherence width of the laser suffices to resolve adjacent Rydberg states? For the typical dye lasers used, the answer is yes. The laser pulse is coherent for times equal or longer than it takes the electron to complete an orbit. Under typical conditions, i.e., a cw excitation of almost all levels except just below the ionization threshold, the principal quantum number n is therefore well defined.

The orientation quantum number m_l is well defined as long as the problem has cylindrical symmetry. The question is therefore whether the angular momentum l of the electron is sharply defined or whether one should use parabolic variables or neither. The dc field splits each degenerate n level into a so-called Stark manifold,[62] whose width in energy is $3n^2F$. Since 1 a.u.$=5.142\times10^9$ V/cm, the width is $1.28\times10^{-4}n^2F$ cm^{-1} for the field strength in V/cm. For the fields of interest, the width of the Stark manifold exceeds the laser coherence width. (Indeed, the Stark manifolds of adjacent n's will overlap.[28,62]) For very high Rydberg states, the laser will not create a coherent superposition of all states of the manifold. The spacing of adjacent states within the manifold is $(3/2)nF$ so that the laser will not excite a particular parabolic state either. Rather, the typical conditions are that a fraction of the Stark manifold is significantly excited. In terms of the ensemble of initial conditions it means that one should use a distribution over I_ξ and I_η, such that their sum is constant. The conjugate angle variables will not be random but will have a distribution with a width smaller than 2π. Equivalently, l will not have a sharp value but will be distributed and its conjugate angle will be nonrandom.

The results reported below are that such distinctions are important but only on a time scale shorter than the recurrence time, $2\pi/(3nF)$, of the Stark manifold. For longer times, the precise initial conditions matter not. While we shall demonstrate the point by the results of the dynamical simulation, it is worthwhile to examine the physical mechanism for this. For this purpose consider the dynamics of l in the presence of a field. Beginning with some initial value, the magnitude of l (to first order approximation in the field) will oscillate with the Stark frequency $3nF$. ($1.28\times10^{-4}nF$ cm^{-1} for the field strength in V/cm or a period of $260.4/nF$ ns). The amplitude of the oscillation depends on m_l and can be as high as $n-1$. Once l has completed more than one period, its particular initial value matters far less. The details of the excitation matter therefore only for the short time dynamics which is about over by $260.4/nF$ ns, for a field strength in V/cm. If, during that time, the principal quantum number n has not changed due to the coupling to the core. Beyond that time, the Rydberg state has sampled almost all its available phase space and its subsequent decay will be kineticlike.

There are two reasons why we are primarily interested in the time evolution of Rydberg states for times longer than the recurrence time of the manifold in phase space of given n and m_l. The first is the pragmatic one that the time resolved experiment is 'blind' during this time. Only such Rydberg states that survive for longer times are detectable. This is a purely practical reason and designs which will reduce the early time detection to about 30 ns are already on the drawing boards. The more fundamental reason is that one expects only a limited coupling to the core during the recurrence time. This is a point to which we will return in detail in Sec. IV D below. The essential point is that the point of closest approach of the electron to the core is $n^2(1-(1-l(l+1)/n^2)^{1/2})$ (which for $l<n$ is well approximated by $l(l+1)/2$ a.u.). Only very low l electrons are therefore coupled to the core. Initially, the value of l is low, whether it is sharply defined or is distributed. During the first recurrence period, only those trajectories where the initial values of the angle variables are such that the electron is initiated on a point on its elliptical orbit which is near the perihelion and moving towards it, will manifest close coupling to the core. For all other initial conditions, l will begin to increase, so that the electron will not feel the core until l decreases again, and that takes the recurrence time. In other words, the approximation that during its first sampling of the available phase space the Rydberg state has well defined n and m_l values is a realistic one. Only a small fraction of all possible initial conditions are given the option to change n during the first round over phase space. Even then, passage close to the core does not guarantee a change in n, it only makes it possible.

For longer times, n can and does change. It changes, both up and down in value, due to the exchange of energy and angular momentum with the core. This can bring it so high up that, due to the lowering of the threshold to ionization, by the presence of the field, it will ionize. The change in n can also drive it down to such low values that it will fail to ionize by the delayed dc field employed for the detection of those Rydberg states that survived. We turn next to a discussion of these two limits.

D. The detection window

By the detection window we mean the range of Rydberg states that are detected as such. The specification of the upper limit is almost unambiguous. The reason is that at the high n values in question, once the electron begins to escape, its value of n rises very rapidly in time. Two points need however to be noted. Strictly speaking, whether an electron with a finite value of n will or will not ionize, is not a function of n only. Rather[28] it depends on the particular values of the actions of the two parabolic variables ξ and η. If the action of the ξ motion is rather high in value, the electron will not ionize even when its total energy is above the minimum classical threshold for ionization at a given n. The reason is that the energy is in the wrong direction, a direction along which the motion is subject to an attractive potential. In the absence of coupling to the core, the parabolic action variables are constants of the motion so that a classical electron, in a Coulombic field, will remain forever bound. Tunneling out is not a practical option[28] because the barrier is so very broad that the tunneling rate is rather slow. In other words, the fraction of Rydberg states that will ionize in a given weak dc stray field is not[28] a step function of the energy of the electron.

The coupling to the core brings about an exchange of energy between the two parabolic coordinates so that, ultimately, all electrons that are above the classical threshold will indeed ionize. But ultimately can be a long time because at the extremely high n's in question, the orbital period is so very long, and the energy exchange can take place only once per orbit. There is a very small fraction of such rather long lived trajectories, but it is not zero.

The second reason why the concept of ionization is not simply defined is that, like in unimolecular dissociation,[63] it is only when the electron is very far from the core that one can be sure that it has indeed ionized. Otherwise, the electron can begin to depart on a hyperbolic orbit but is recaptured into a bound orbit by the interaction with the core.[64] Such capture processes have indeed been documented in the scattering of very low energy electrons by larger molecules.[65] The action-angle variables are not easily extended into the continuum and it requires a different set of variables to smoothly span the boundary between the bound and continuum motion.[66]

In this paper we take the electron to have ionized when its principal action variable is larger than the value needed for ionization by the dc stray field, and it rapidly increases further. The numerical examples will illustrate that this rise provides a rather clean signature.

The lower end of the detection window is more problematic to define in a strict fashion. Operationally, this is the lowest value of n which the delayed field ionization detector will recognize as a Rydberg state. The narrower width of the Stark manifold at lower n's makes the determination of the required numerical value quite simple. The direct approach is to regard the Rydberg state as having undergone an internal quenching once the value of n has gone down below that point. The counter argument is that the coupling to the core can, sooner or later, drive the value of n back up. Experimentally one does detect a second and longer living component of Rydberg states. We have previously[12] suggested, on the basis of a kinetic analysis, that the second component is indeed due to those states which have gone sufficiently down in n and are therefore not detectable as Rydberg states, but which have subsequently come back up into the detection window. The proposed[12] mechanism is then that the states of n below the detection window serve as a reservoir which can repopulate those states which are detectable as Rydbergs.

The trajectory results, cf. Fig. 10 below, are very consistent with the interpretation that states can come back up in n. Yet the situation is not as simple as we may wish it to be. The first problem is that at lower n's the amplitude of the oscillation in l is much reduced, cf. Sec. III A below, so that the electron is much more frequently in the vicinity of the core. Another reason is that, in a real polyatomic molecule there are many vibrational modes which can couple effectively with the lower n electron,[33,67] drain its energy further, and thereby, de facto, preclude its ever gaining enough energy to come back up. In the simulations there is only one vibrational mode. We have therefore used two alternative procedures. In the first one, once n decreased below the detection limit the trajectory is counted as having decayed down. This way one obtains rather clean, essentially single exponential kinetic decays. The rate of this process is what we shall report as the rate of decay down. In the second procedure, we continue to follow the trajectory in time, up to 4 μs. If during that time the trajectory recrosses the lower end point of the detection window, we take the Rydberg state to have resurrected. This does yield a second and longer time component, Fig. 10 below, just as anticipated by the kinetic analysis.[12] A further caveat is, however, in order. The time scale of the second component is such that, in an actual experiment, one cannot rule out a contribution due to collisional effects to the experimentally observed kinetics. All that one can state with confidence is that there can be also a purely intramolecular origin for the long time stability. We return to these points in Sec. V below.

III. DYNAMICS

This section presents both computational results and analytical considerations for the time evolution of high Rydberg states, in the presence of a weak dc stray field. The discussion will refer to the following observations[18] about the dynamics in the field free case: While the electrical anisotropy of the core is not very short ranged, on the scale of a high n Rydberg orbit, its effect is significant only when the electron is very near the core, where the velocity of the electron is highest. On the time scale of the orbital period, the change in the action variables of the electron due to the coupling to the core is essentially instantaneous, and occurs at or very near to the point of closest approach. The new feature in the present study is the role of the dc field, whose effect persists throughout the orbit. This will lead us to the introduction of the time stretch caused by the presence of the field. The limits on the regime in n and field strength within which the time stretch is operative will be spelled out. Due to the coupling to the core, the energy of the electron can either increase or decrease. The net result is that a bound Rydberg trajectory either terminates when an electron escapes by ion-

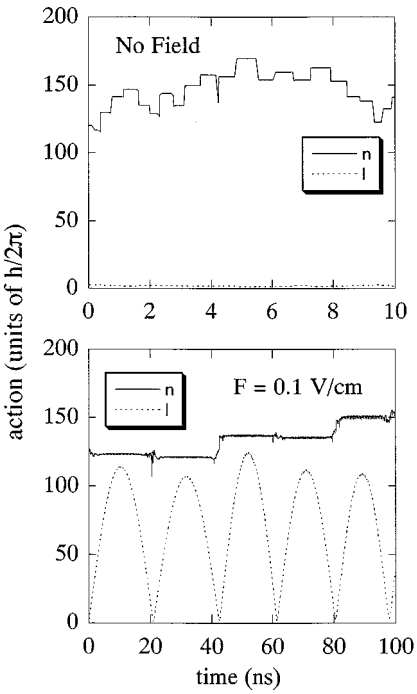

FIG. 1. The principal action, n, and the orbital angular momentum, l (both in units of $\hbar$) of a high Rydberg electron revolving around an anisotropic ionic core, vs time, in the absence (top panel) and presence (bottom panel) of a weak dc field. In the absence of a field, n changes once per revolution, when the electron is near the core. At the point of closest approach the velocity of the electron is high so that the period of the orbit is quite long as compared to the time spent near the perihelion. The changes in n appear therefore to be instantaneous on the time scale shown, which spans over a dozen periods. In the presence of the field, the orbital momentum of the electron oscillates (bottom panel) with a harmonic frequency proportional to n and to the field strength F. The example shown corresponds to the situation typical of the high n case, when the period of the l motion is longer than the orbital period so that the electron executes several revolutions for every oscillation of l. During those time intervals when l is high, the electron will not get near the core and so n will not appreciably change during that orbit. The result is that in the presence of the field, the changes in n are less frequent (by a factor of about 1/15, in the case shown) as compared to the field free case. This is the time stretch due to the dc field.

ization (the so-called[5] up decay channel) or by the energy decreasing sufficiently that the state will escape detection (the down decay channel).

A. The time dilution

Figure 1 compares the time evolution of the principal action n and the angular momentum l in two trajectories with *identical* initial conditions. The difference is the presence or absence of a weak dc field in the Hamiltonian. By plotting both sets of results on a common time scale it is very evident that in the presence of the field, the change in n is slowed down. The reason for this is clearly revealed in the oscillatory time dependence of the angular momentum l. For much of the time, l is large and thereby prevents the electron from getting too near to the core. [Recall that the distance of closest approach at lower l values is $l(l+1)/2$.] During the times when l is large the electron is decoupled from the core. On the other hand, l does periodically decrease, at which times the electron gets kicked by the core just as if there is no dc field present. In other words, the electron–core coupling is on for only a fraction of the time. The magnitude of this fraction is the time interval for which l is small compared to the period of the overall oscillation in l. From a kinetic point of view, the time is slowed down, by the same fraction.

From a quantum mechanical point of view, the oscillation is due to the initial state not being a Stark or parabolic eigenstate of the Hamiltonian including the field. Rather, it is a superposition of eigenstates with time varying coefficients, where the variation is due to the small energy differences between the states of the Stark manifold. Indeed, we have already noted the equivalence between the period of classical oscillation of l and the recurrence time for sampling the Stark manifold of states. It follows that the stretch of the time axis is just as valid in quantum mechanics. To prepare an initial state with a rather narrow distribution of l values requires, as we have seen in Sec. II C, a laser whose coherence width spans all, or almost all, of the Stark width. Our laser is narrower, but as we shall argue in Sec. III B below, this matters only at times of the order of the recurrence time. In the present study, we are interested in longer times where, cf. Fig. 15 below, the time evolution is no longer sensitive to the initial phases.

The time dilution discussed above is the same effect as discussed in the theory of radiationless transitions.[26,68,69] The physical origin of the small but finite spacing of eigenstates is, of course, quite different, as are other details, but the essence of the phenomena is the same. An increase in the lifetime of high Rydberg states of diatomic molecules due to an imposed electrical field has indeed been reported by Bordas *et al.*[24,51] and interpreted as due to the quantum mechanical dilution effect.

The time scale of the decay of the Rydberg state due to the coupling to the core is stretched because the coupling is switched on only during a fraction of every cycle of the oscillation of l. Since most electrons survive for many such oscillations, the net result is that the kinetic time is stretched inversely to the fraction of the time during which the electron can couple to the core. A simple estimate is obtained by taking the coupling to the core to be effective when $l<l_0$ where l_0 is small, $l_0<n$. Then the fraction is l_0/n and the stretch is n/l_0. A longer derivation is to note that when l is small it changes linearly with time, as can be seen by expanding $n\sin(\omega t)$ near the origin, where ω is the frequency of the l motion. Then, with $\omega=3nF$, the time during which $l<l_0$ is $l_0/3n^2F$ or l_0/n per revolution of l.

The argument above assumes that the period of oscillation in l is higher than the period of the orbital motion of the electron. Then, it is only on those occasions that the electron returns to the vicinity of the core and l is low that the coupling will be effective. Because the dc field is weak this is the normal case in our problem. When l oscillates faster than the orbital motion it can no longer preclude a close approach of the electron to the core. The frequency of the l oscillation is $3nF$ so that this is a high field or a high n limit. The high end of the time stretch occurs when the frequency $3nF$ is larger than the orbital frequency n^{-3} (the spacings of adjacent Rydberg states) or

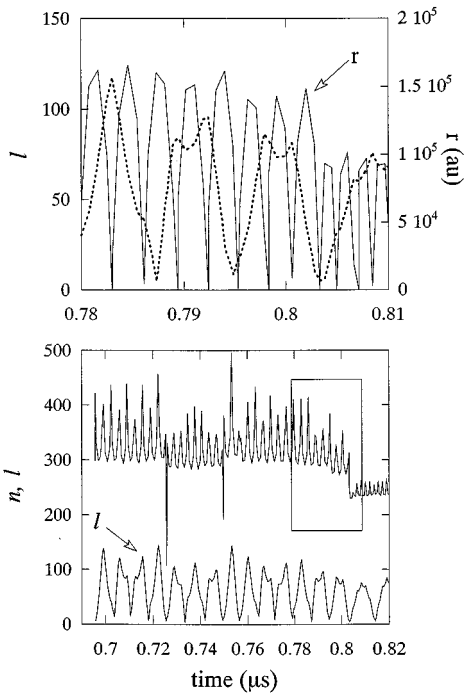

FIG. 2. A short time segment of a trajectory for a very high value of n, in the presence of a dc field. This trajectory is near the high end limit, Eq. (3.1), where the period of oscillation of l is almost as short as the orbital period, bottom panel. Note that for this trajectory m_l is finite (i.e., l does not decrease all the way to zero) so that the amplitude of the l oscillation is less than n. The top panel shows l (dashed line) and the radius of the Bohr–Sommerfeld orbit vs time. Note that the l motion is not quite harmonic. Only when l and r are simultaneously small, can a large change in n occur (one such case at $t \approx 0.803$ μs, is emphasized by a frame in the bottom panel). The fast oscillations in the value of n as seen in the bottom panel are due to n not being quite a good quantum number.

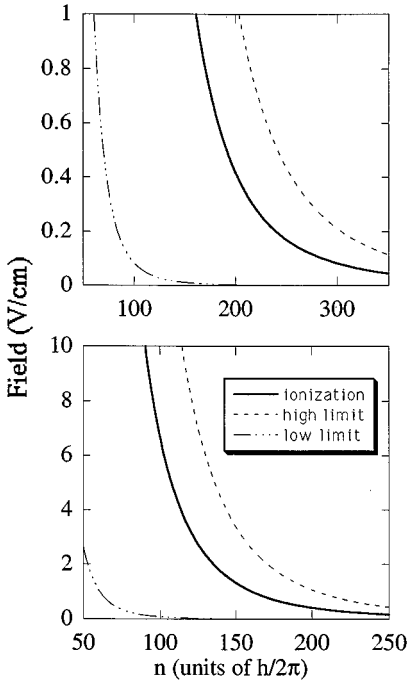

FIG. 3. A plot of the dc field strength, in V/cm vs the principal action n showing the boundaries of the high end, Eq. (3.1), and low end, Eq. (3.2), limits. Also shown in the classical threshold for ionization in the presence of the field. Not all electrons can ionize at threshold (Ref. 28), cf. Fig. 6 below, but even so, we do not expect the high end to be realized. (But one can get near to it, cf. Fig. 2). The low end limit is particularly relevant to series of high quantum defects. (The actual boundary shown is drawn for a quantum defect of 0.3). For realistic field strengths as used in ZEKE type experiments the low end is, very roughly, at $n=100$. We intend to explore in more detail whether the low end as discussed is the boundary between the lower n and higher n regimes, compare Figs. 1 and 2 above to Figs. 4 and 5 below.

$$3n^4F \geqslant 1, \quad \text{high end.} \tag{3.1}$$

This limit corresponds to a very extensive overlap of the Stark manifolds of adjacent n states. Indeed an equality in Eq. (3.1) roughly matches the criterion for the value of the field necessary to ionize a state of given n (the onset is at[28] $n^4F=0.13$). The high end can be approached but not reached. In Sec. III B below we shall show how one can approach the high end for low values of the parabolic action variable I_η. It will also become evident that the sojourn at the high end can last for no more than a dozen or so orbits of n after which the electron will ionize.

Figure 2 shows details of a trajectory near the high end, Eq. (3.1), for an initial value of $n=150$. Note how the period of the oscillation in l is now much shorter than in Fig. 1 and is comparable to the orbital period. (The upper panel shows both l and the position of the electron. In this plot one can see the second order effect which causes the l motion to be anharmonic. The maximal value of l is below n because the value of m_l is finite). During the propagation of the trajectory in time, n increased and, in the time segment shown, it comes even closer to the high n end. It is, however, only when l and r are simultaneously small that n does change in a significant fashion. (See inset in the lower panel.) The very fast oscillations in n are due to it being not a good quantum number since we use the definition of the hydrogenic n, see Appendix A.

There is also a lower limit due to the precession of the orbit of the electron. This motion is due[4,48] to the non-Coulombic terms in the central potential in which the electron moves and corresponds to a rotation of the long and short axes of the orbit. When the precession is very rapid, it can counteract the effect of the field (which can be thought of as acting on a dipole with a magnitude $I_\xi - I_\eta$). The frequency of the precession depends on the r dependence of the non-Coulombic term. For a potential which varies as C_2/r^2 the change in angle of the axes is[4,48] $2\pi m_e C_2/l^2$ per revolution, where m_e is the mass of the electron. The frequency of precession is $(C_2/l^2)/n^3 \equiv \delta/n^3$ in atomic units, where δ is the quantum defect.[4] The change in angle over the time when l is small is $(\delta/n^3)\cdot(l_0/3n^2F)$ and the low end is when that change is large so that, before the field can act on l, the electronic dipole has turned away

$$3n^5F/\delta l_0 < 1, \quad \text{low end, dipolar coupling.} \tag{3.2}$$

For lower values of n one expects therefore that the kinetic time will run faster. The onset of the low end can be somewhat shifted to higher values of n by an increase in the applied field, Fig. 3. The trajectory simulations unambigu-

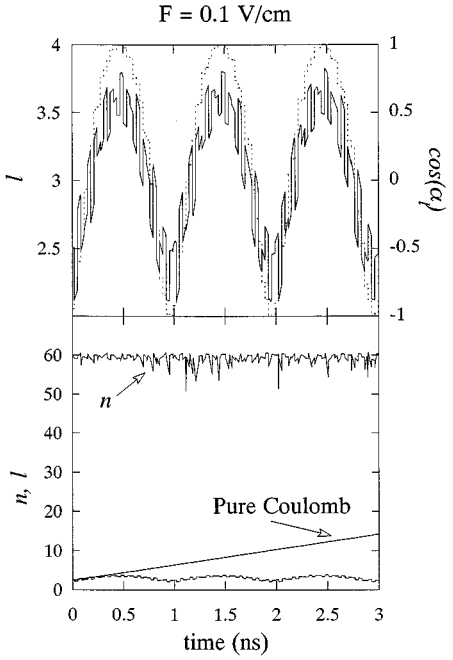

FIG. 4. A time segment of a trajectory in the presence of a field showing the role of the precession of the orbit in switching off the time stretch. The results are for an initial $n=60$ in the presence of a dc field of 0.1 V/cm and for $C_2=0.3$ so that the trajectory is below the low end defined by Eq. (3.2). The upper panel shows l, (solid line) and the angle made by the long axis of the trajectory, which should be constant if there was no precession of the orbit. The bottom panel shows n and l vs time. Unlike the trajectories which are above the low end, cf. Figs. 1 and 2, the amplitude of l remains low. To emphasize that it is the precession of the orbit that keeps l from oscillating, we turned off the non Coulombic part of the central potential seen by the electron, all other parameters remaining the same. The resulting plot of l vs time is also shown in the bottom panel, labeled pure Coulomb limit. The increase in l is very evident. (For $n=60$, the period of the l oscillation is long so only part of the cycle is seen in the plot).

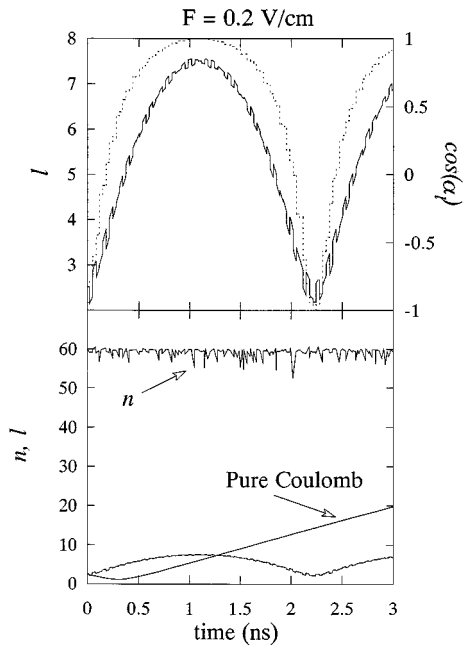

FIG. 5. Same as Fig. 4 but for a twice higher field strength. Note the doubling of the period and the amplitude of the oscillations in l. In a future experiment we intend to scan through the boundary of the low end so as to examine the onset of a high n behavior.

ously manifest the low end limit. Figures 4 and 5 show results for $n=60$ at two dc field strengths. At the lower field, the frequency of the precession is comparable to the frequency ω of the oscillation in l (upper panel). The magnitude of l does not oscillate much. For a somewhat higher field, the amplitude of the l oscillation is higher, but is still low enough to allow an uninterrupted coupling of the electron to the core, as seen in Fig. 5, which is drawn for initial conditions just below the low end limit.

Experimental work is needed to establish the relevance of the low end regime. What the theoretical considerations do, however, indicate that for molecules with a high quantum defect, Rydberg states up to quite high n's will decay much faster (i.e., on an essentially field-free time scale[18]) because the amplitude of the oscillation of the orbital angular momentum of the electron will remain low even in the presence of a field, cf. Figs. 4 and 5. We consider that DABCO may well be an example of that class and discuss the point further in Sec. V.

B. Dynamics using parabolic action variables

The parabolic action variables change in time only due to the electron–core coupling (term V) cf. Eq. (2.4). A trajectory with given initial value of the parabolic action variables can correspond to an entire range of values of l and the particular value is determined by the values of the angle variables. During the trajectory, as the angle variables change, so does the value of l. The time stretch as discussed before is just as valid and, as the results below will show, once the time is past the recurrence period, the dynamics looks essentially the same whether the initial conditions are specified by the hydrogenic or the parabolic actions. In quantum mechanics, two such initial states are quite different. A state of given n, l is a linear combination of parabolic, I_ξ, I_η states and vice versa.[60] During the first recurrent time, the small energy spacing lead to differences in the time evolution due to quantum beats. For longer times, the phase factors will defacto randomize, partly due to the interactions with the core, whether such that only cause a phase shift or those that induce transitions. The essential point which we emphasized throughout is that the interesting dynamics occur on a time scale long compared to the recurrence time of the Stark manifold.

The parabolic variables do provide an interpretation of why some trajectories take longer than others to ionize. Figure 6 shows a trajectory where, for much of the time $I_\xi > I_\eta$. During that time the value of n reaches rather high values so that the energy of the electron is above the threshold for ionization in the presence of the stray dc field. Yet ionization does not take place because much of the energy is in the ξ motion, which is bound. Also shown in Fig. 6 is the opposite case where $I_\eta > I_\xi$. It is important to re-emphasize that the parabolic action variables are conserved only in the absence of coupling to the core and therefore that eventually an electron which is above the classical threshold for ionization will

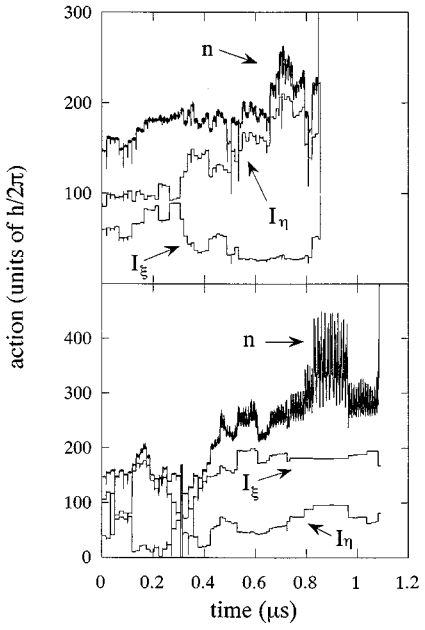

FIG. 6. The time evolution of the parabolic action variables during a trajectory where the total energy is above the classical threshold for ionization in the presence of the dc field. The motion along the direction ξ is bound. Hence, as long as the energy (which we measure by the action variable I_ξ) in the ξ motion is high, the electron will not ionize even when its instantaneous n value exceeds the threshold for ionization which is at $n=300$. A time segment where this is the case is evident in the lower panel. It requires energy in the η motion for the electron to exit. The coupling to the core mixes the two motions so that ultimately the electron does ionize. The extra kinetic stability conferred in this way does not however last for very long, cf. Fig. 15.

ionize. Delayed ionization of so-called Stark states which are above the classical threshold for ionization is also known in atoms.[56,57] The origin of the stability, as discussed here, is the same as in atoms. The difference, evident in Fig. 6, is that, here, the ultimate decay is due to the anisotropy of the core and is accompanied by a large change in n. Also (as will be shown in Fig. 15, the decay can be either up or down.

It is not likely that a high initial value of I_ξ provides a mechanism for very long time stability. Even at quite high n's (say, 350, which can be ionized in fields above 0.05 V/cm), where the orbital period can reach tens of ns's, it takes no more than a dozen or so revolutions of l for the ξ and η motions to exchange quanta so that the resulting delay is typically in the sub-μs range. What the discussion in this section does, however, provide is the reason why, in an ensemble of trajectories of given n, and in the presence of a weak dc stray field, there is, for times longer than 100 ns or so, a decay which is only dependent on the initial value of n and not on any other details of the excitation process.

The discussion above and the results of Sec. IV below point out to a need to significantly shorten the onset time of the detection scheme. It is only then that one could really probe the details of the dynamics. Alternatively, one could try to lengthen the time necessary for the sampling of the ensemble of initial conditions. One possibility is to operate under such conditions that not only l but also m_l are not conserved. The stretch of the time axis will then scale as n^2 and the recurrence time will increase accordingly. Since $l \geqslant |m_l|$ this will also have the effect that even at high n's, most trajectories, will, most of the time, decouple the electron from the core with a consequent long time stability. Such initial excitation requires the destruction of the cylindrical symmetry during the excitation process, a symmetry which does obtain for a dc field in a given direction.

IV. KINETICS OF THE DECAY

This section reports the time evolution of the number of surviving Rydberg states, i.e., states within the detection window as a function of the weak dc field. The experimental results on the role of the dc field are for a particular initial state in DABCO while the computations also examine different ensembles of initial conditions. Any given ensemble corresponds at least to 200 trajectories which are followed in time until the first exit from the detection window (but see also Fig. 10 below) or up to 4 μs. The upper limit of the detection window is taken to be above the threshold for ionization to insure that all states that can ionize are accounted for. The lower limit is put at $n=90$ which corresponds to a delayed detection field of about 11.5 V/cm, except as otherwise noted. The implication is, of course, that using a stronger dc field for detection will, at a given initial n, reveal more Rydberg states. This is the case for aromatic molecules[14] (but is not the case for DABCO). Moreover, lower n values, which for a given delayed field appear to decay too rapidly to be observed after the experimentally imposed 100–200 ns start time of the observation, will give rise to a signal when the detection field is increased. It would, however, be better to make the experimental test for a higher dc field so as to lower the value of n at which a low end behavior, cf. Eq. (3.2), sets in. The experimental verification of both of these expectations regarding the role of the detection field, provides what we regard as definite evidence for the importance of the down decay channel.

Typical comparisons of experiment and computations are shown in Figs. 7 and 8. Figure 7 demonstrates the concept of the time stretch. A presently computed decay is superimposed on the results of computations in the absence of a dc field. The results are quite similar except that the time scales differ by a factor of 20. Figure 8 shows a comparison between experimental results (for BBC) and the present computations. It is evident that the long time decay is not well accounted for in such computations that regard all electrons whose n value drops below the bottom end of the detection window as being lost forever. We return to this point in Fig. 10 below and, in more detail, in Sec. V.

A. The up and down decay channels

The original proposal[5] was that the short time decay of a high molecular Rydberg state occurs via one of two competing channels. The up route is ionization while the down route is due to the lowering down of the value of n below the detection limit. It was further proposed that the two decay channels have a branching ratio which is strongly n dependent. Low initial n's decay primarily by the down route while high initial n's preferentially ionize. A subsequent ki-

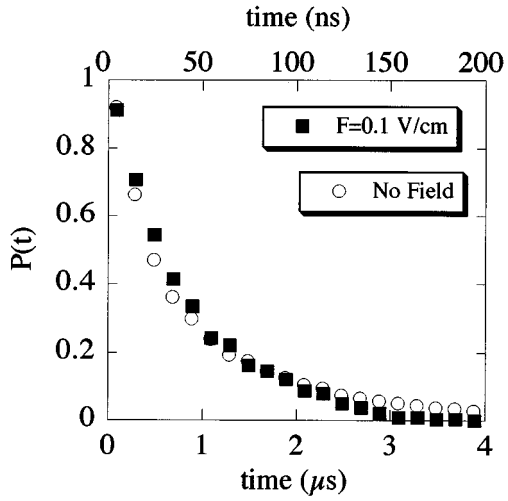

FIG. 7. Computed decay kinetics in the absence and presence of the field. Shown in the computed fraction of trajectories which have remained in the detection window up to the time t, vs time in μs. Computed for an initial value of $n=135$ and a rotational constant $B=0.15$ cm^{-1}. The bottom time scale is for the computation in the presence of a field of 0.1 V/cm. The time scale for the results in the absence of the field is given in the upper scale. Note the stretch factor of about 20. In the text we argued that the time stretch is n/l_0 where l_0 is the cutoff angular momentum for the electron core coupling. The results shown are equivalent to $l_0 \approx 8$ which is consistent with the results obtained for the time history of a trajectory computed for such an initial value of l.

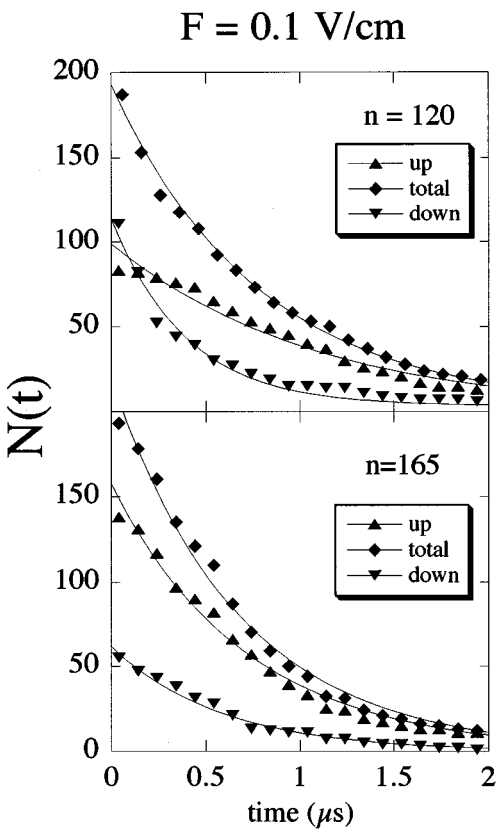

FIG. 9. The decay kinetics for two initial values of n. The trajectories are classified according to their ultimate fate. For the lower initial n, the majority of the trajectories decay down, i.e., their value of n decreased below the lower end of the detection window. (Note that in this figure, once this happened, the trajectory is assumed to have permanently decayed, never to return. A different convention is adopted in Fig. 10, where the trajectories are allowed to continue to propagate whatever their value of n is). For the higher initial n, most trajectories decay up, i.e., by ionization. The figure verifies our original proposal (Ref. 1) that the maximal, vs frequency, lifetime of the high Rydberg states is due to a switch over in the mechanism of the decay. At early times, the decay is not exponential. In the text this induction time is interpreted as the time necessary for the sampling of the initially available phase space.

netic analysis[12] of experimental data verified that the branching is independent of the background rare gas.

Figure 9 contrasts the computed decay curves for two values of n which straddle the turnover point between the two mechanisms. It is obtained by running an ensemble of initial conditions and recording the ultimate fate of each trajectory. In this way, one can report the numbers of the trajectories that will decay by either the up or the down route and that have survived up to the time t. It is very clear from the simulations, both in the presence and absence[18] of the field, that both decay channels contribute and that their relative contribution does change in an n-dependent manner. It is also clear from the figure (lower panel) that there is an induction time of about 100 ns before a kinetic regime is established. We have argued above that this time is the time needed for the bound system to sample its available phase space. The argument is very similar to the one commonly used in RRKM theory[70] to justify the concept of a unimolecular rate constant which is only dependent on the total energy of the molecule and is independent of the initial mode of excitation. In a preliminary account of this work[26] we have provided kinetic evidence that, past the initial induction time, the two decay channels are competing, that is that there is one population which decays either up or down. As the discussion above shows, this is the case because the resampling of phase space is faster than either decay (whose rates, at high n's, are in the hundreds of ns's), so that the population is always re-equilibrated on the scale of the decay. Else-

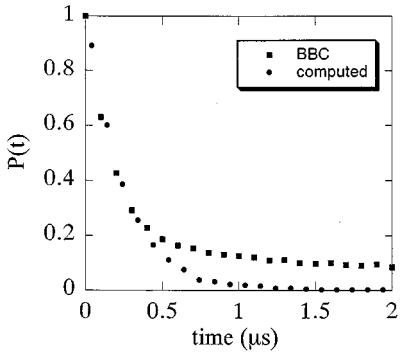

FIG. 8. Comparison of observed (for BBC at an excitation energy of 6 cm^{-1} below the ionization continuum) and computed (for a diatomic core at an initial $n=150$ and a dc field of 0.5 V/cm) decay kinetics. Shown in the fraction of states that survived in the detection window up to the time t. The purpose of the drawing is to show that the experiment and computations yield comparable time scales for the fast decay and that the present computations fail to account for the long time component. No optimization of the computations was attempted and the rotation constant of the core and all other details of the computation are as in all other figures shown in this paper.

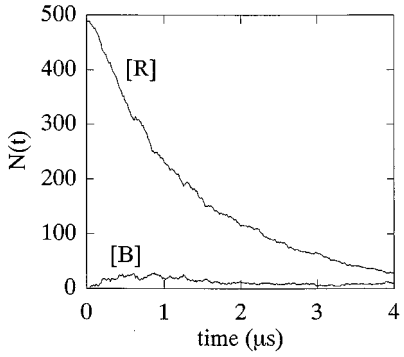

FIG. 10. The decay kinetics when account is taken of the reservoir states (Ref. 12). All trajectories are propagated for 4 μs unless they ionize first. $[R]$ is the fraction of trajectories that survive in the detection window up to the time t. (The detection window is the range of states that will be detected as Rydberg states by the ZEKE type ionization in a delayed field.) $[B]$ is the fraction of trajectories that, at the time t, have a value of n below the lower end of the detection window, which is at $n=90$. These are the reservoir states and they can either couple to the vibrations and thereby decay further or their n value can increase and they can return to the detectable range. The resurrection of the reservoir states is a possible intramolecular route for long time stability. (Compare the long time tail in $[R]$ to the computed decay in Fig. 8.) Inspection of Fig. 17 below will show that the number, $[B]$ of reservoir states will be quite a bit higher for a higher value of the bottom end of the detection window. ($n=90$, as used in this figure corresponds to a delayed field of 11.5 V/cm).

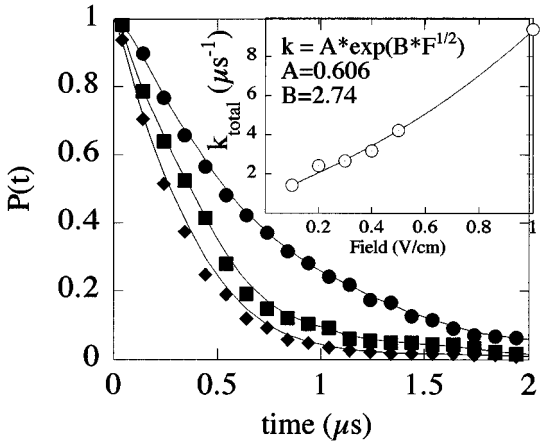

FIG. 11. The effect of the dc field of the computed decay kinetics. Shown are three curves (the fit is to an exponential decay) of the fraction of Rydberg states that survived up to the time t vs time. Note the faster decay at higher field strengths. Computed for an initial $n=150$. The results of the fit are shown as a decay rate vs field plot in the inset. The fit therein serves two purposes. The first is to identify the prime reason for the field dependence of the decay rate. Our initial proposal[1] was that the rate is exponentially small in the energy required to ionize the electron. The field lowers this energy by $\approx 4\sqrt{F}$ and the fit shown is to an exponential dependence on $\sqrt{F}$. The second point is the need to determine the time stretch factor. The field dependence of the decay rate requires that we extrapolate the rate to zero field and only then compare to the rate computed in the field free case. As discussed in the text, this yields a stretch factor of ~ 20.

where we will provide a rederivation of this picture using a different approach.

Past the induction time, the decays shown in Fig. 9 are essentially a single exponential. The fits shown allow for a long time component, which is found to be 1% or less of the initial population. Note, however, that the classification into alternative decay channels is based on a detection window where once the value of n drops below 90 it is assumed to have decayed for ever. This is not unreasonable for large molecules where the density of vibrational states rapidly increase with energy. Therefore, once electronic to vibrational exchange of energy takes place, the electron is unlikely to regain its energy. This will be particularly true in molecules such as DABCO where it is known[13,33(b),67] that the lower Rydberg states predissociate. The prime emphasis in this paper is therefore on the first exit from the detection window. On the other hand, one is familiar with, so called, ''inverse electronic relaxation''[45,69,71] in which a substantial fraction of the vibrational energy content of the ground state of a polyatomic molecule is being converted to electronic energy. It is therefore not possible to rule out the possibility that an electron regains its energy. Figure 10 examines this point by not terminating the integration at the first exit. Rather, Fig. 10 shows the results when trajectories are followed in time for 4 μs or until they ionize, whichever comes first.

The analysis of the trajectories shown in Fig. 10 follows the scheme used to examine[12] the experimental data. That is, a trajectory is counted as being in the detection window during such times that its value of n is $90<n<1000$. The fraction of such trajectories is denoted by $[R]$ as in the kinetic analysis.[38] When $n<90$, the trajectory is counted as being in a reservoir state which will not be detected. The fraction of such trajectories at a given time is denoted as $[B]$. Otherwise, the trajectory is taken to have ionized (the value of 1000 for the upper limit of the detection window is not critical. Once the electron is on its way out, n changes so very rapidly that any reasonable estimate will do. We checked that the results are unchanged when the upper cutoff is as low down as 350 or as high as 2000). As is clear from the figure, (and from Fig. 17 below), there is, as in the kinetic analysis[12] of the experimental data, a gradual accumulation of trajectories in the reservoir states and that, after a while, these trajectories do wander back into the detection window. The net result is a longer time component in the decay, due to the repopulation of detectable Rydberg states. We do not have overwhelming evidence that this is the origin of the observed long time stability. It is even likely that this cannot be the right explanation for molecules with a high quantum defect for which the onset of the low end condition, Eq. (3.2), occurs at higher values of n. We do have clear cut evidence that this is a viable route, particularly so, in such molecules where the coupling to the vibrations is weak. It may not be the only way, it may not be the major way, but it is definitely a way. More on this, in Sec. V.

B. The role of the dc stray field

Increasing the strength of the stray dc field lowers the threshold for ionization. It should therefore shorten the lifetime in that electrons can ionize at a lower value of n (recall that the diabatic threshold is at[28] $4\sqrt{F}$ cm^{-1} for F in V/cm). As should be expected on the basis of the argument that both the up and the down channels compete and as will be discussed in Sec. IV E below, the presence of the field is mani-

TABLE I. Computed decay rates (in μs^{-1}) vs the principal action n for three values of the dc field.

	n	$F=0.1$ V/cm	$F=0.3$ V/cm	$F=0.5$ V/cm
0	100.00			
1	110.00		2.1200	2.1800
2	120.00	1.3000	2.0000	2.6000
3	135.00	1.2200	2.4200	3.1100
4	150.00	1.4300	2.6600	4.1200
5	165.00	1.4900	2.5500	4.6400
6	180.00	1.4800	3.1100	5.4600
7	200.00	1.7900	3.9000	

fested also in the down process. Beyond this, the field affects the dynamics in that the magnitude of l oscillates, as discussed in Sec. III A. For the weak stray fields that are likely in a realistic setup (say, <0.2 V/cm), and for high n's, one is typically between the high and low ends, cf. Fig. 3, so that the time stretch is about independent of the magnitude of the field.

Figure 11 shows the decay curves computed at three different values of the field. To exhibit the faster decay at higher fields, all curves are normalized to a common value of unity at the origin of the time axis. The decay is essentially single exponential and the rates increase from 1.4 μs^{-1} at $F=0.1$ V/cm to 8.6 μs^{-1} at 1.0 V/cm. The field dependence of the overall decay rate is very closely approximated (insert in Fig. 11) by an exponential increase with the lowering of the threshold for ionization.[1] The extrapolation to zero field yields a rate of 0.6 μs^{-1} as compared to 13.5 μs^{-1} for a computation[18] of the decay rate in the field free case for the same Hamiltonian parameters. The difference is due to the extrapolated value being for a stretched time. The computations in Fig. 11 are for $n=150$ and the factor of 20 between the two rates is a direct measure of the time stretch. It corresponds to a cutoff angular momentum of the electron–core coupling $l_0 \approx 8$, which is very reasonable.

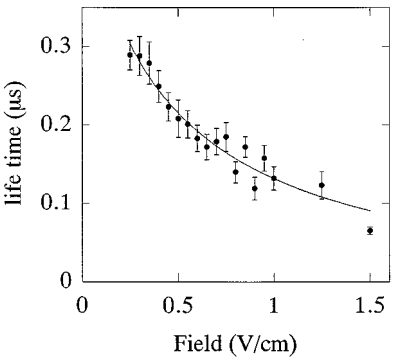

FIG. 12. The experimental determination of the lifetime, in μs, of the fast decay in DABCO (at an excitation energy of 7 cm^{-1} below ionization. Other details as in Ref. 13) vs the externally imposed dc field strength in V/cm. Each point corresponds to a separate decay curve. (These are not shown but are very similar to the result shown for BBC in Fig. 8). The stray dc field in our experiment is estimated to be below 0.2 V/cm and this is consistent with the results shown. The experimentally observed slower decay (not shown) is also faster when a field is imposed and with a rather similar field dependence. This is consistent with the intramolecular mechanism for this decay, as discussed in the legend to Fig. 10.

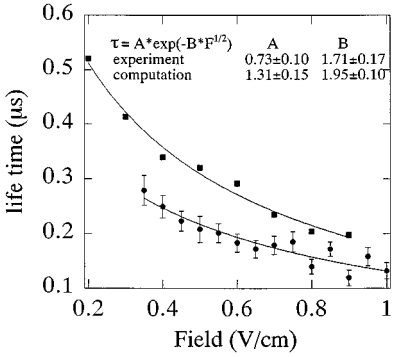

FIG. 13. A comparison of the experimental and the computed effect of the dc field on the lifetime of the fast decay. Experimental results (full circles) for DABCO, from Fig. 12. Computed results (squares) for an initial $n=135$. The comparison is two fold, as shown in the inset and is based on the fit discussed for Fig. 11. The extrapolation to the zero field limit shows that the computed decay is slower, but note that no attempt was made to fit the experimental results and that the computed results shown are as in Ref. 26. The dependence on the magnitude of the dc field, for the two sets of results, is similar.

Table I provides a summary of the effect of the dc field on the decay rates for a range of initial values of n.

C. Experimental and computational results

Figure 12 is a summary of the experimental results for a particular high Rydberg state in DABCO. Shown is the lifetime vs the dc field. The increase in the decay rate with the increasing field, cf. Fig. 11 is very evident. The fit shown is as in Fig. 11. (In addition to the imposed dc field there is an unavoidable stray component. It is estimated to be below 0.2 V/cm and this estimate is consistent with the plot as all but the lowest point fall on a smooth curve.) Figure 13 compares the dc field dependence of the experimental as well as the computed lifetimes. It is clear that the computations capture both the magnitude of the time scale and the effect of the field.

The comparison shown in Fig. 13 is based on the premise that the short time decay in DABCO is similar to that of the other molecules we studied. We have every reason to think that this is the case. The point is that the high Rydberg states of DABCO are pumped via a vibrationally excited state (excess energy of ca. 1000 cm^{-1}) of the S_1 intermediate state and that the low Rydberg states of DABCO are known to undergo a facile predissociation.[67] In a preliminary experiment, we have verified that the short time decay is essentially independent of the excess vibrational energy (in the range of 500 to 1400 cm^{-1}) of the intermediate state. Additional conclusions must await the completion of our, in progress, trijoint very high frequency resolution/time resolution/computational study of the role of the vibrations of the core.

Figure 14 shows the variation of the total decay rate, which is the only rate which can be directly measured or computed, vs n. [Past the initial induction time, the up and down decay channels are competing,[26] cf. Eqs. (4.1)–(4.4).]

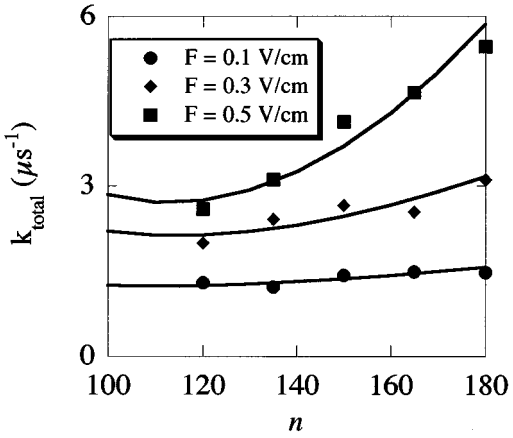

FIG. 14. The variation of the computed decay rate with the initial value of n, at different field strengths. The curves shown are just to guide the eye. In a forthcoming study we will propose an analytical approximation which will enable us to justify the scaling with n.

The minimum in the decay rate vs. n, observed already in the very first experiments[1] is evident and is only very weakly field dependent. In these computations the lower end of the observation window is taken to be at $n=90$. The decay rate is faster so that the computed effect of the dc field is more marked if the lower end of the detection window is lowered, cf. Fig. 17 below.

D. Decay kinetics for parabolic initial conditions

When the initial ensemble is specified in terms of given values of the parabolic action variables, there is a distribution of initial values of the angular momentum of the electron. This does affect the early time dynamics but, as is should be expected from the discussion in Sec. II C, the longer time dynamics are governed essentially only by the initial value of n. Figure 15 shows a typical decay curve. These, and similar results for other initial energies, verify that the role of the initial distribution of l values is manifested primarily during the first recurrence period.

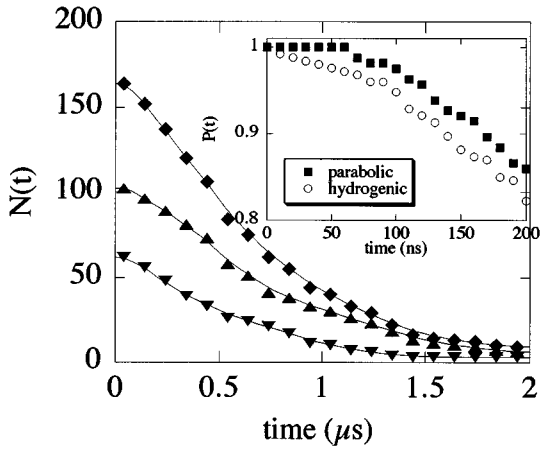

FIG. 15. Decay kinetics for an ensemble of trajectories specified by given initial values of the parabolic actions, computed for a dc field of 0.1 V/cm. In the absence of a field the initial state used is equivalent to $n=150$ so that the results are to be compared to the lower panel in Fig. 11. To emphasize the role of the Stark splitting, which offers the possibility of a coherent excitation, we provide a detailed comparison in the inset. Shown is the very early time kinetics of the present ensemble vs. that for an ensemble where the initial values of n and l are sharply defined. As discussed in the text, there is a difference but only for times of the order of the recurrence time of the Stark manifold. For much longer times one cannot discern the role of the details of the initial excitation. The results are for an example that emphasizes the differences because, as can be seen in the inset, the initial values of the parabolic actions chosen confer a short time stability (cf. the legend to Fig. 6) and for other choices the differences will be smaller.

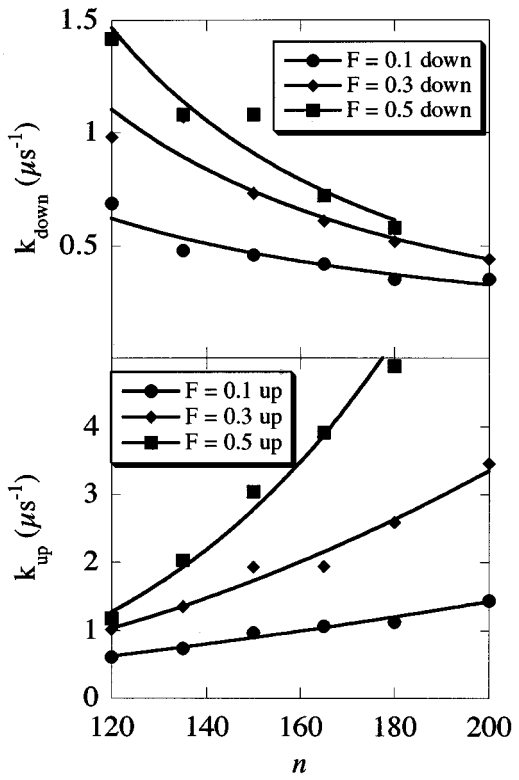

FIG. 16. The branching fractions for the down and the up processes vs the initial value of n at several field strengths. The initial energy is as, if not more, important than the value of the field in determining the ultimate fate of the trajectory. This result is to be expected since the field lowers the threshold to ionization by only $\approx 4\sqrt{F}$ cm^{-1}. The branching ratio of the down processes decreases with increasing field because trajectories which for a weaker field will eventually go down can, at stronger fields, ionize first. The rate constants for the up and the down processes, defined by Eqs. (4.1)–(4.4), are obtained by multiplying the total decay rate, Fig. 14, by the branching fractions.

To analyze the role of a distribution of l values, note that the cutoff angular momentum, l_0, for electron core coupling is smaller than n. Therefore,[28] for given values of I_ξ and I_η, most initial conditions correspond to such l values that the electron is initially decoupled from the core. The first effect is that there are far fewer ionization events where the electron escapes within the first revolution around the core. However, since in the absence of the field,[18] such prompt ionization results from but a very small fraction of the possible initial conditions, this effect is not very dominant. The other effect is that the induction time prior to the sampling of l values due to the dc fields is more noticeable, cf. Fig. 15. Since this time is short compared to the time at which the experiment can begin to monitor the decay, this too is not of operational importance. In other words, at current experi-

mental capabilities we cannot point out to a clear experimental signature of the particular initial conditions accessed in the experiment. Such, of course, will not be the case if during the initial excitation one can destroy not only the conservation of l but also of m_l. This point has already been noted in Sec. III B and will be retaken up by us in a future publication.

E. The up/down branching ratio

The presence of the dc field lowers the threshold for ionization and is therefore expected to favor the up process. The effect is clearly noticeable, Fig. 16, but is not large. The results, shown as a branching fraction vs. n, demonstrate that the initial value of n is more important in determining the branching ratio with the result that the turnover point between the two decay channels is only weakly field dependent. To examine the relevant factors, we note that[26] the three populations, those states that decay down, those that decay up and the total population, all have a common decay constant. This is, of course, the signature of a competitive decay. This, total, decay constant k_{total} can, however, be written as a sum of rate constants, for the up and the down transition in the manner suggested by the kinetic decay schemes shown in Eqs. (4.1)–(4.4)

$$\frac{d[R]}{dt}=d([R_{\text{up}}]+[R_{\text{down}}])/dt=-(k_{\text{up}}+k_{\text{down}})[R], \tag{4.1}$$

$$[R_{\text{up}}]=(k_{\text{up}}/k_{\text{total}})[R]=(k_{\text{up}}/k_{\text{total}})[R]^0\ \exp(-k_{\text{total}}t), \tag{4.2}$$

$$[R_{\text{down}}]=(k_{\text{down}}/k_{\text{total}})[R]=(k_{\text{down}}/k_{\text{total}})[R]^0 \times\exp(-k_{\text{total}}t), \tag{4.3}$$

$$k_{\text{total}}=(k_{\text{up}}+k_{\text{down}}). \tag{4.4}$$

The results for the rates are obtainable from Fig. 16. One finds that both rates are increased by the presence of the field, but that, as a function of n, the effect is in opposite direction for the up and the down channels. The higher is the initial value of n, the larger is the effect of the field on k_{up} and vice versa for k_{down}. Since the dc field lowers the energy threshold for ionization, its effect on k_{up} is to be expected.[1] The field effect on k_{down} is indirect. Trajectories which at lower field strengths would wander up and down in n, now ionize as soon as n gets to higher values and are denied the option to decay down. The decay down therefore occurs sooner, the higher the dc field and hence k_{down} increases.

V. COMMENTS ON LONG TIME STABILITY

For times longer than necessary to sample the initially available phase space, and for absorbing conditions at the lower end of the detection window, the computed kinetics of the decay of an initial ensemble are essentially exponential, into two competing channels. The rate depends only on the initial energy of the electron and on the strength of the stray dc field, which we take to be constant from the excitation up to the detection. The differences in the dynamics between parabolic states of the same value of n but different values of I_ξ and I_η average out when an ensemble of initial conditions is examined and for times longer than the sampling time of the initially available phase space. All these results are very consistent with the experimental results on the shorter, sub-μs time scale, major component of the decay. There appears however no obvious intramolecular mechanism for endowing the system with longer term stability, which in our experiments comprise about 5%–15% of the total decay. A nonconservation of m_l could, in principle, provide a viable route, but we found no way (apart from a non space fixed dc stray field at the time of excitation), that would cause a sufficient coupling of states of different m_l's. (Of course, collisions with external perturbers[6,7] particularly if ionic, would easily induce such reorientation.[72] We are also still looking for a way to make the core itself anisotropic enough to do it. What is clear is that a much larger core, where the effective scale of its anisotropy is larger. $(l_0(l_0+1)/2)\approx 50$ a.u. will suffice. That, however, is more than is reasonable for a typical sized aromatic molecule but not unreasonable for a peptide.[64]

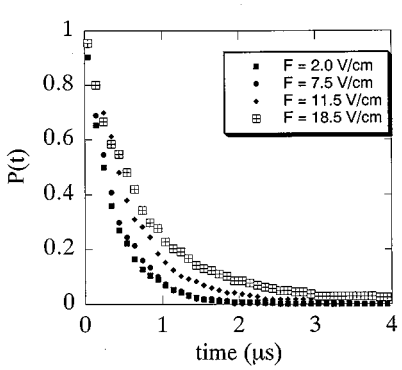

FIG. 17. Computed decay curves for different detection windows. The detection window is defined so that its low end is the threshold for ionization by the delayed dc field used for detection. The value of this field is shown in the inset. (Not to be confused with the dc field imposed from the very start). It is very clear that lowering the low end of the detection field recovers more Rydberg states. Note that a wide range of low ends is covered. At $F=2$ V/cm, states below $n=140$ escape detection while for $F=18.5$ V/cm, the low end is at $n=80$. Another view of the effect of the lower end of the detection window is provided in Fig. 10. That figure was computed for a low end at $n=90$.

It appears therefore that the long term stability is intermolecular in origin[6,7] and/or can be due to the intramolecular mechanism that we originally proposed,[12] namely, that there is a reservoir of high, but not very high, Rydberg states that are below the detection window. These states are populated by the down transitions but can repopulate the states higher up, Fig. 10. (The reservoir states have values of n which are too low to be detected by the delayed dc field.) Obviously, the importance of external perturbers depends on the particular experimental conditions[6,7,73] but the present results suggest that an intramolecular route cannot be ruled out at this time. Experiments along the lines of Refs. 6,7,16,22,73 will eventually lead to a resolution of this point. Of particular interest in this connection are experiments on molecules which exhibit efficient conversion of electronic to vibrational energy[13] as the return up of the reservoir states is likely to be reduced in such systems, with predissociation being the ultimate dominant fate of the down transitions.

The computational evidence for reservoir states is summarized in Fig. 17. It shows (for $n=150$ and a weak dc field of 0.1 V/cm) a series of decay curves computed for increasing values of the delayed field used for detecting the surviving Rydberg states. The fields shown correspond to varying the lower end of the detection window from $n=140$ down to $n=80$. The decay rate obviously decreases with the lowering of the bottom end of the detection because states which for a lower delayed field are out of the reach of detection and therefore are not counted as surviving Rydberg states, are inside the detection window at higher fields. Figure 17, taken together with Fig. 10, suggest to us that there can be reservoir states. The experimental evidence on this point is not, at the moment, clear cut. The observed decay kinetics in both BBC and DABCO exhibit a long time component, as do the earlier results for the aromatic molecules. These are observed at an amplitude of 5%–15% even for low delayed fields (such that the lower end of the detection window is at $n=\sim 100$), whereas at such fields our computed long time component is smaller. At the moment, the question of a possible intramolecular mechanism for a long time stability is open.

VI. CONCLUDING REMARKS

The experimental–theoretical–computational evidence presented in this paper suggests that in the absence of other external perturbations the prime role of a dc field is to scale down the decay time of high Rydberg states. The mechanism is the slow, on the time scale of the electron's orbital period, oscillation in the magnitude of l. When the period of these oscillations is so slow that it is comparable to the time of precession of the orbit, the time stretch ceases. This is the boundary between the intermediate and high Rydberg states. Otherwise, the magnitude of the stretch is n/l_0 where l_0 is the lowest orbital angular momentum which allows the electron to get near enough to the core. The computed decay kinetics show a short induction time during which the details of the initial excitation matter. It lasts for about the recurrence time of the available phase space. Our currently available time resolution is not short enough to examine this interesting regime. At longer (but still, sub-μs) times, there is good agreement between the observed and computed decay, and on the effect of the dc field on it. Many questions remain, however, open. Mostly they are related to the, lower amplitude, longer time (μs scale) decay component, which is of prime interest for ZEKE spectroscopists. Others concern the role of the vibrations of the core and the importance of predissociation, particularly so for highly vibrationally excited cores.[11] In terms of the energy scale, an experimental open problem is the time resolved behavior in the region of not very high Rydberg states (say n of 50 to 100) a region of interest because the oscillation of l will be particularly fast compared to the orbital period so that the effect of time stretch is expected to disappear. Work is in progress on many of these points.

ACKNOWLEDGMENTS

We thank Professor R. Bersohn, Professor J. Jortner, Professor E. W. Schlag, and Professor R. N. Zare for discussions, advice, and encouragement and the referee for her/his comments. This work was supported by the Stiftung Volkswagenwerk and the German–Israel James Franck Binational Program. A.M. is a Minerva fellow. E.R. is a Clore Foundation scholar. The Fritz Haber Research Center is supported by MINERVA.

APPENDIX A: ACTION-ANGLE VARIABLES

This Appendix provides the technical details on the variables which are used to integrate Hamilton's equations of motion.

1. Hydrogenic action angle

This section follows Born.[4] The Hamiltonian for a hydrogeniclike electron written in polar coordinates is, in atomic units

$$H=\frac{1}{2}\,(p_r^2+p_\theta^2/r^2+p_\phi^2/r^2\,\sin^2(\theta))-\frac{1}{r}. \tag{A1}$$

Using a canonical transformation,[4,70] three actions n, l, m_l and their conjugated angles α_n, α_l and α_{ml} replace r, θ, ϕ and their conjugated momenta p_r, p_θ, p_ϕ. n is the classical analog of the principal quantum number. l is the action of the angular momentum and m_l is its projection the z axis. The position vector of the electron is related to the action-angle variables by the introduction of an auxiliary variable u, known as the eccentric anomaly

$$r=n^2\cdot(1-\epsilon_n\cdot\cos(u)). \tag{A2}$$

u is connected to α_n by the implicit equation

$$\alpha_n=u+\epsilon_n\cdot\sin(u). \tag{A3}$$

α_n is taken to be equal to zero at the outer turning point. ϵ_n determines the ellipicity and is related to n and l

$$\epsilon_n=(1-l^2/n^2)^{1/2}. \tag{A4}$$

The polar angle θ is related to the action-angle variables by the introduction of another auxiliary variable ψ, which is related to the standard polar representation of an ellipse [see Eq. (A7) below]

$$\cos(\theta)=\sin(\beta_l)\cdot\cos(\alpha_l+\psi). \tag{A5}$$

β_l determines the orientation of the ellipse with respect to the z axis

$$\cos(\beta_l)=m_l/l. \tag{A6}$$

The standard polar representation of an ellipse is

$$r=\frac{\rho(1-\epsilon_n^2)}{1+\epsilon_n\cdot\cos(\psi)}. \tag{A7}$$

Using the above definitions we can relate the polar angle ϕ, and the three momenta p_r, p_θ, p_ϕ to the action-angle variables

$$\sin(\theta)\exp(\pm i\phi) = -[\cos(\beta_l)\cdot\cos(\alpha_l+\psi) \pm i\ \sin(\alpha_l+\psi)]\exp(\pm i\alpha_{m_l}), \quad \text{(A8)}$$

$$p_r = -\frac{(n^2-l^2)^{1/2}\ \sin(u)}{n^2(1+\epsilon_n\cdot\cos(u))}, \quad \text{(A9)}$$

$$p_\theta = \frac{l(l^2-m_l^2)^{1/2}\ \sin(\alpha_l+\psi)}{[l^2\ \sin^2(\alpha_l+\psi)+m_l^2\ \cos^2(\alpha_l+\psi)]^{1/2}}, \quad \text{(A10)}$$

$$p_\phi = m_l. \quad \text{(A11)}$$

In the action-angle representation the Hamiltonian depends only on the action n

$$H = 1/2n^2. \quad \text{(A12)}$$

The three actions n, l, and m_l and the two angles α_l, and α_{ml} are all constants of the motion.

2. Linear rigid rotor

The rotation of the molecule is described by a linear rigid rotor. In this section we describe the canonical transformation from a polar representation (θ, ϕ, and their conjugate momenta p_θ, p_ϕ) of a two dimensional linear rigid rotor to an action-angle representation. The Hamiltonian in polar coordinates is given by Eq. (A13):

$$H = B(p_\theta^2 + p_\phi^2/\sin^2(\theta)). \quad \text{(A13)}$$

B is the rotational constant. The corresponding Hamilton–Jacobi equation yield the relation between the new canonical action-angle variables j, m_j, α_j, α_{mj} and the polar variables. j is the action of the total angular momentum of the rigid rotor and m_j is its projection on the z axis. The relation between the polar variables and the action-angle variables is

$$\cos(\theta) = (1-m_j^2/j^2)^{1/2}\ \cos(\alpha_j), \quad \text{(A14)}$$

$$\phi = \alpha_{m_j} + \arctan[(j/m_j)\cdot\tan(\alpha_j)] - \pi, \quad \text{(A15)}$$

$$p_\theta = \frac{j(j^2-m^2)^{1/2}\ \sin(\alpha_j)}{[j^2\ \sin^2(\alpha_j)+m_j^2\ \cos^2(\alpha_j)]^{1/2}}, \quad \text{(A16)}$$

$$p_\phi = m_j. \quad \text{(A17)}$$

The inverse of the trigonometric function is being chosen to increase around the orbit. The Hamiltonian in the new canonical variables depends only on the total angular momentum j, leading to a conservation of the two action j, m_j, and the angle α_{mj}

$$H = Bj^2. \quad \text{(A18)}$$

3. Morse oscillator

The vibration of the molecule is described by a one dimensional Morse oscillator. The variables R, P are replaces by the action i which is the analog of the quantum number of the vibration and its conjugate angle α_i, the phase of the oscillator. The zero of α_i is taken at the inner turning point. Equations (A19)–(A20) describe the relation between the two sets of canonical variables

$$R = R_e + \beta^{-1}\ \ln[(1+\sqrt{\epsilon_i}\ \cos(\alpha_i))/(1-\epsilon_i)], \quad \text{(A19)}$$

$$P = (2mD_e)^{1/2}[\epsilon_i(1-\epsilon_i)]^{1/2}\ \sin(\alpha_i)/(1-\sqrt{\epsilon_i}\ \cos(\alpha_i)). \quad \text{(A20)}$$

D_e is the depth of the Morse potential and β is the range parameter. m is the reduce mass of the vibrating molecule. The Hamiltonian has the form

$$H = P^2/2m + D_e(1-\exp(-\beta(R-R_e))) = \beta^{-1}(2D_e/m)^{1/2}i - (\beta^2/2m)i^2, \quad \text{(A21)}$$

where

$$\epsilon_i = \beta^{-1}(2/mD_e)^{1/2}i - (\beta^2/2mD_e)i^2. \quad \text{(A22)}$$

APPENDIX B: PARABOLIC ACTION VARIABLES

This Appendix provides the working expressions needed to compute the parabolic action-angle variables. The primary reference is again Born.[4]

The Hamiltonian of a hydrogenlike electron in a constant dc electric field can be written in parabolic coordinates

$$H = [2\cdot(\xi^2+\eta^2)]^{-1}[p_\xi^2 + p_\eta^2 + (\xi^{-2}+\eta^{-2})p_\phi^2 + F(\xi^4-\eta^4) - 4]. \quad \text{(B1)}$$

The relation between the parabolic coordinates and the Cartesian/polar coordinates is

$$x = r\ \sin\ \theta\ \cos\ \phi = \xi\eta\ \cos\ \phi,$$
$$y = r\ \sin\ \theta\ \sin\ \phi = \xi\eta\ \sin\ \phi, \quad \text{(B2)}$$
$$z = r\ \cos\ \theta = (\xi^2-\eta^2)/2.$$

One can obtain[4,48] (to first order in the field F) the relation between the parabolic action variables I_η, I_ξ, and I_ϕ and the hydrogenic action-angle variables by introducing the separation constants (x_1, x_2 such that $x_1+x_2=2$)

$$I_\eta = 0.5[-m_l + x_2/(-2E)^{-1/2} - 0.25F(-2E)^{-3/2}\times(m_l^2+1.5x_2^2/E)], \quad \text{(B3)}$$

$$I_\xi = 0.5[-m_l + x_1/(-2E)^{-1/2} + 0.25F(-2E)^{-3/2}\times(m_l^2+1.5x_1^2/E)], \quad \text{(B4)}$$

$$I_\phi = m_l, \quad \text{(B5)}$$

E being the energy of the electron in the presence of the field. In terms of the hydrogenic action-angle variables E takes the form (see Appendix A)

$$E = -1/2n^2 + Fn^2\cdot(1-\epsilon_n\cdot\cos(u))\sin(\beta_l)\cos(\alpha_l+\psi), \quad \text{(B6)}$$

or in parabolic action-angle variables (to first order in the field F)

$$E = -(1/2)(I_\xi+I_\eta+I_\phi)^2 - (3/2)F(I_\xi+I_\eta+I_\phi)(I_\xi-I_\eta). \quad \text{(B7)}$$

The separation constants (x_1,x_2) are related to the parabolic coordinates and their conjugated momenta

$$x_1 = \xi(2p_\xi^2 + p_\phi^2/2\xi^2 + F\xi/2 - E),$$
$$x_2 = \eta(2p_\eta^2 + p_\phi^2/2\eta^2 - F\eta/2 - E). \quad \text{(B8)}$$

In order to complete the picture the relation between the parabolic momenta and the polar momenta (derived using the hydrogenic action variables of Appendix A) is

$$p_\xi = p_r/2 - [2r(1+\cos\theta)]^{-1}\sin\theta p_\theta,$$
$$p_\eta = p_r/2 + [2r(1-\cos\theta)]^{-1}\sin\theta p_\theta, \quad \text{(B9)}$$
$$p_\phi = p_\phi(\text{hydrogenic}) = m_l.$$

[1] E. W. Schlag, W. B. Peatman, and K. Müller-Dethlefs, J. Elect. Spectrosc. **66**, 139 (1993).
[2] K. Müller-Dethlefs and E. W. Schlag, Ann. Rev. Phys. Chem. **42**, 109 (1991).
[3] F. Merkt and T. P. Softley, Int. Rev. Phys. Chem. **12**, 205 (1993).
[4] M. Born, *Mechanics of the Atom* (Blackie, London, 1951).
[5] D. Bahatt, U. Even, and R. D. Levine, J. Chem. Phys. **98**, 1744 (1993).
[6] W. A. Chupka, J. Chem. Phys. **99**, 5900 (1993).
[7] Xu Zhang, J. M. Smith, and J. L. Knee, J. Chem. Phys. **99**, 3133 (1993).
[8] (a) F. Merkt, H. H. Fielding, and T. P. Softley, Chem. Phys. Lett. **202**, 153 (1993); (b) F. Merkt, J. Chem. Phys. **100**, 2623 (1994); (c) F. Merkt and R. N. Zare (to be published).
[9] P. Debye, Phys. Z. **20**, 160 (1919); J. Holtsmark, *ibid*. **25**, 73 (1924).
[10] *Rydberg States of Atoms and Molecules*, edited by R. F. Stebbings and F. B. Dunning (Cambridge University, Cambridge, 1983).
[11] W. G. Scherzer, H. L. Selzle, E. W. Schlag, and R. D. Levine, Phys. Rev. Lett. **72**, 1435 (1994).
[12] U. Even, M. Ben-Nun, and R. D. Levine, Chem. Phys. Lett. **210**, 416 (1993).
[13] U. Even, R. D. Levine, and R. Bersohn, J. Phys. Chem. **98**, 3472 (1994).
[14] D. Bahatt, Ph.D. thesis, Tel-Aviv University, 1993.
[15] D. Bahatt, O. Cheshnovsky, U. Even, N. Lavie, and Y. Magen, J. Phys. Chem. **91**, 2460 (1987).
[16] D. Bahatt, O. Cheshnovsky, and U. Even, Z. Phys. D **40**, 1 (1993).
[17] U. Even, to be published. In the parallel plate arrangement one can have the lower end of the detection window down to $n=70$.
[18] E. Rabani, R. D. Levine, and U. Even, J. Phys. Chem. **98**, 8834 (1994).
[19] (a) F. Merkt and T. P. Softley, Phys. Rev. A **46**, 302 (1992); (b) F. Merkt and T. P. Softley, J. Chem. Phys. **96**, 4149 (1992).
[20] G. Reiser, W. Habenicht, K. Müller-Dethlefs, and E. W. Schlag, Chem. Phys. Lett. **152**, 119 (1988).
[21] G. P. Bryant, Y. Jiang, M. Martin, and E. R. Grant, J. Phys. Chem. **96**, 6875 (1992).
[22] H. Krause and H. J. Neusser, J. Chem. Phys. **97**, 5932 (1992); *ibid*. **99**, 6278 (1993).
[23] R. S. Freund, in Ref. 10.
[24] W. G. Alt, Scherzer, H. L. Selzle, and E. W. Schlag, Chem. Phys. Lett. **224**, 366 (1994).
[25] C. Bordas, P. F. Brevet, M. Broyer, J. Chevaleyre, P. Labastie, and J. P. Petto, Phys. Rev. Lett. **60**, 917 (1988).
[26] E. Rabani, L. Ya. Baranov, R. D. Levine, and U. Even, Chem. Phys. Lett. **221**, 473 (1994).
[27] E. W. Schlag and R. D. Levine, J. Phys. Chem. **96**, 10668 (1992).
[28] L. Ya. Baranov, R. Kris, R. D. Levine, and U. Even, J. Chem. Phys. **100**, 186 (1994).
[29] R. S. Berry, J. Chem. Phys. **45**, 1228 (1966).
[30] J. N. Bardsley, Chem. Phys. Lett. **1**, 229 (1967).
[31] U. Fano, J. Opt. Soc. Am. **65**, 979 (1975).
[32] C. H. Greene and Ch. Jungen, Adv. Atom. Mol. Phys. **21**, 51 (1985).
[33] (a) R. L. Whetten, G. S. Ezra, and E. R. Grant, Annu. Rev. Phys. Chem. **36**, 277 (1985); (b) M. Ito, T. Ebata, and N. Mikami, *ibid*. **39**, 123 (1988).
[34] (a) J. Chevaleyre, C. Bordas, M. Broyer, and P. Labastie, Phys. Rev. Lett. **57**, 3027 (1986); (b) C. Bordas, M. Broyer, J. Chevaleyre, and P. Labastie, J. Phys. (Paris) **48**, 647 (1987).
[35] M. S. Child and Ch. Jungen, J. Chem. Phys. **93**, 7756 (1990).
[36] K. Müller-Dethlefs, J. Chem. Phys. **95**, 4821 (1991).
[37] H. Nakamura, Int. Rev. Phys. Chem. **10**, 123 (1991).
[38] R. D. Gilbert and M. S. Child, Chem. Phys. Lett. **287**, 153 (1991).
[39] S. T. Pratt, J. Chem. Phys. **98**, 9241 (1993).
[40] (a) B. V. Chirikov, Phys. Rep. **52**, 263 (1979); (b) G. M. Zaslavsky, *ibid*. **80**, 157 (1981).
[41] J. Jortner and R. D. Levine, Isr. J. Chem. **30**, 207 (1990).
[42] R. D. Levine and R. B. Bernstein, *Molecular Reaction Dynamics* (Oxford University, London, 1974).
[43] G. E. Ewing, J. Phys. Chem. **91**, 4662 (1987).
[44] J. A. Beswick and J. Jortner, Adv. Chem. Phys. **47**, 363 (1981).
[45] J. Jortner and R. D. Levine, Adv. Chem. Phys. **47**, 1 (1981).
[46] W. A. Chupka, J. Chem. Phys. **98**, 4520 (1993).
[47] M. Bixon and J. Jortner, J. Chem. Phys. **48**, 715 (1968).
[48] L. D. Landau and E. M. Lifshitz, *Mechanics*, 3rd ed. (Pergamon, Oxford, 1976).
[49] M. S. Child, *Semiclassical Mechanics with Molecular Applications* (Clarendon, Oxford, 1991).
[50] Ch. Jungen and O. Atabek, J. Chem. Phys. **66**, 5584 (1977).
[51] C. Bordas, P. Labastie, J. Chevaleyre, and M. Broyer, Chem. Phys. **129**, 21 (1989).
[52] N. Y. Du and C. H. Greene, J. Chem. Phys. **85**, 5430 (1986).
[53] A. L. Roche and Ch. Jungen, J. Chem. Phys. **98**, 3637 (1993).
[54] L.-S. Wang, J. Conceicao, C. Jin, and R. E. Smalley, Chem. Phys. Lett. **182**, 5 (1991); P. G. Datskos, L. G. Christophorue, and J. G. Carter, *ibid*. **195**, 329 (1992); C. C. Han and J. I. Brauman, J. Phys. Chem. **94**, 3403 (1990); K. E. Salomon and J. I. Brauman, *ibid*. **92**, 6948 (1998).
[55] U. Fano and A. R. P. Rau, *Atomic Collisions and Spectra* (Academic, Orlando, 1986).
[56] H. Rottke and K. H. Welge, Phys. Rev. A **33**, 301 (1986).
[57] V. V. Kolosov, J. Phys. B **22**, 1989 (1989).
[58] C. W. Gear, The Numerical Integration of Ordinary Differential Equations of Various Orders, Report ANL 7126, Argonne National Laboratory, 1966.
[59] W. H. Press, B. P. Flannery, S. A. Teukolsky, and W. T. Vetterling, *Numerical Recipes in C* (Cambridge University, New York, 1988).
[60] D. Park, Z. Phys. **159**, 155 (1960).
[61] M. Nauenberg, Phys. Rev. A **40**, 1133 (1989); J.-C. Gay, D. Delande and A. Bomier, *ibid*. **39**, 6587 (1989).
[62] D. Kleppner, M. G. Littman, and M. L. Zimmerman in Ref. 10.
[63] G. G. Hall and R. D. Levine, J. Chem. Phys. **44**, 1567 (1966).
[64] E. W. Schlag, H. J. Grotemeyer, and R. D. Levine, Chem. Phys. Lett. **190**, 521 (1992).
[65] (a) H. S. Carman and R. N. Compton, J. Chem. Phys. **98**, 2473 (1993); (b) D. Smith, P. Spanel, and T. D. Märk, Chem. Phys. Lett. **213**, 202 (1993); (c) P. G. Datskos, L. G. Christophorou, and J. G. Carter, J. Chem. Phys. **98**, 7875 (1993).
[66] L. Ya. Baranov and R. D. Levine (to be published).
[67] (a) M. Fuji, T. Ebata, N. Mikami, and M. Ito, Chem. Phys. Lett. **101**, 530 (1983); (b) G. J. Fisanick, T. S. Eichelberger IV, M. B. Robin, and N. A. Kuebler, J. Phys. Chem. **87**, 2240 (1983); (c) M. Fujii, T. Ebata, N. Mikami, and M. Ito, J. Phys. Chem. **88**, 4265 (1984); (d) M. Fujii, N. Mikami, and M. Ito, Chem. Phys. **99**, 193 (1985).
[68] A. Nitzan, J. Jortner, and P. M. Rentzepis, Proc. R. Soc. London, Ser. A **327**, 367 (1972).
[69] J. Jortner and S. Mukamel, in *The World of Quantum Chemistry*, edited by R. R. Daudel and B. Pullman (Reidel, Boston, 1974), p. 225.
[70] I. Oref and B. S. Rabinovitch, Acct. Chem. Res. **12**, 166 (1979).
[71] A. Nitzan and J. Jortner, J. Chem. Phys. **71**, 3524 (1979).
[72] R. Bersohn and S. H. Lin, Adv. Chem. Phys. **16**, 67 (1969).
[73] C. E. Alt, W. G. Scherzer, H. L. Selzle, E. W. Schlag, L. Ya. Baranov, and R. D. Levine, J. Phys. Chem. (in press).